

correct, its ESR spectrum should have  $g_{\parallel}$  and  $g_{\perp}$  values comparable to the electronically analogous  $\text{Pc}^{2-}\text{Co}^{\text{II}}$  and  $\text{Pc}^{2-}\text{Fe}^{\text{I}}$ . We would also anticipate that such a species should exhibit marked solvent dependence in both its ESR spectrum and its electrochemistry because of the presence of an unpaired electron in the  $z^2$  orbital. Indeed it is most likely to be five-coordinate (low-spin  $d^7$ , cf.  $\text{Pc}^{2-}\text{Fe}^{\text{I}}\text{S}^{3b}$ ). The ESR spectrum of the dianion is in fact very similar to that of the six-coordinate low-spin  $d^6$   $\text{Pc}^{2-}\text{Mn}^{\text{II}}$  precursor. The reversibility observed in the electrochemistry of this species and the absence of any following reaction led us to assume that the coordination number probably remains six with two coordinated solvent molecules. The species is therefore assigned as  $\text{Pc}^{4-}\text{Mn}^{\text{II}}\text{S}_2$ .

### Conclusion

Within the range studied, the manganese phthalocyanine system gives rise to the species  $[\text{Pc}^-\text{Mn}^{\text{III}}\text{S}_2]^{2+}$ ,  $[\text{Pc}^{2-}\text{Mn}^{\text{III}}\text{S}_2]^+$ ,  $\text{Pc}^{2-}\text{Mn}^{\text{II}}\text{S}_2$ ,  $\text{Pc}^{3-}\text{Mn}^{\text{II}}\text{S}_2^-$ , and  $[\text{Pc}^{4-}\text{Mn}^{\text{II}}\text{S}_2]^{2-}$ , where in the case of the manganese(III) species, a solvent molecule may be displaced by an anion X. No evidence of manganese(I) was observed in distinction to the iron and cobalt series.<sup>3,17</sup> The electron-transfer rates of the  $\text{PcMn}^{\text{II}}$  electron-transfer steps are similar in magnitude to those usually found in analogous porphyrin series.<sup>24</sup> Unlike (TPP) $\text{Mn}^{\text{III}}\text{Cl}$ , however, the rate is not profoundly changed by either choice of anion or coordinating ligands. The  $\text{Pc}^{2-}\text{Mn}^{\text{III}}/\text{Pc}^{2-}\text{Mn}^{\text{II}}$  couple appears at a slightly more anodic potential than in the porphyrin

series. Reduction of the phthalocyanine ring, however, to form  $[\text{Pc}^{3-}\text{Mn}^{\text{II}}\text{S}_2]^-$  appears 0.5–0.8 V anodic of the corresponding porphyrin reduction.<sup>25</sup> These trends are consistent with earlier views of the comparative electrochemistry of porphyrins and phthalocyanines.<sup>3,26</sup> This comparison illustrates the variation in coordination electronic and geometric structure accessible within the  $\text{MN}_4$  class of compounds and its effect upon electrochemical properties.

**Acknowledgment.** This is part of a joint investigation with Professor A. J. Bard (The University of Texas at Austin) supported by the U.S. Office of Naval Research, to whom we are indebted. We also thank the Natural Science and Engineering Research Council (Ottawa) for financial support. Finally, we thank Dr. S. Ma for the donation of a sample of (tetra-*tert*-butylphthalocyaninato)manganese(III) hydroxide.

**Registry No.**  $\text{Pc}^{2-}\text{Mn}^{\text{II}}(\text{py})_2$ , 77648-32-9;  $\text{Pc}^{2-}\text{Mn}^{\text{II}}(\text{Me}_2\text{SO})_2$ , 77648-33-0;  $\text{Pc}^{2-}\text{Mn}^{\text{II}}(\text{DMF})_2$ , 77648-34-1;  $\text{Pc}^{2-}\text{Mn}^{\text{II}}(\text{DMA})_2$ , 77661-61-1;  $[\text{Pc}^{2-}\text{Mn}^{\text{III}}(\text{py})_2]^+$ , 77648-35-2;  $[\text{Pc}^{2-}\text{Mn}^{\text{III}}(\text{Me}_2\text{SO})_2]^+$ , 77648-36-3;  $[\text{Pc}^{2-}\text{Mn}^{\text{III}}(\text{DMF})_2]^+$ , 77648-37-4;  $[\text{Pc}^{2-}\text{Mn}^{\text{III}}(\text{DMA})_2]^+$ , 77648-38-5;  $[\text{Pc}^{3-}\text{Mn}^{\text{II}}(\text{py})_2]^-$ , 77648-39-6;  $[\text{Pc}^{3-}\text{Mn}^{\text{II}}(\text{Me}_2\text{SO})_2]^-$ , 77648-40-9;  $[\text{Pc}^{3-}\text{Mn}^{\text{II}}(\text{DMF})_2]^-$ , 77648-41-0;  $[\text{Pc}^{3-}\text{Mn}^{\text{II}}(\text{DMA})_2]^-$ , 77648-42-1;  $[\text{Pc}^{4-}\text{Mn}^{\text{II}}(\text{py})_2]^{2-}$ , 77661-62-2;  $[\text{Pc}^{4-}\text{Mn}^{\text{II}}(\text{Me}_2\text{SO})_2]^{2-}$ , 77648-43-2;  $[\text{Pc}^{4-}\text{Mn}^{\text{II}}(\text{DMF})_2]^{2-}$ , 77648-44-3;  $[\text{Pc}^{4-}\text{Mn}^{\text{II}}(\text{DMA})_2]^{2-}$ , 77648-45-4;  $[\text{Pc}^-\text{Mn}^{\text{III}}(\text{DMF})_2]^{2+}$ , 77648-46-5.

(25) Boucher, L. J.; Garber, K. *Inorg. Chem.* 1970, 9, 2644.

(26) Lever, A. B. P. "Abstracts of Papers", First Chemical Congress of the North American Continent, Mexico City, Mexico, 1975; American Chemical Society: Washington, D.C., 1975; INOR 028.

(24) Kadish, K. M.; Davis, D. G. *Anal. N.Y. Acad. Sci.* 1973, 206, 495.

Contribution from the Department of Chemistry,  
McGill University, Montreal, Quebec, Canada H3A 2K6

## Vibrational Spectra and Potential Constants of the Pentacarbonyl(chalcocarbonyl)metal(0) Complexes $\text{M}(\text{CO})_5(\text{CX})$ ( $\text{M} = \text{Cr}, \text{W}$ ; $\text{X} = \text{S}, \text{Se}$ )

ANN M. ENGLISH, KEITH R. PLOWMAN, and IAN S. BUTLER\*

Received July 3, 1980

Vibrational spectra have been recorded at ambient temperatures for the five chalcocarbonyl complexes  $\text{Cr}(\text{CO})_5(\text{CS})$ ,  $\text{Cr}(\text{CO})_5(\text{S})$ ,  $\text{Cr}(\text{CO})_5(\text{CS})$ ,  $\text{Cr}(\text{CO})_5(\text{S})$ , and  $\text{Cr}(\text{CO})_5(\text{CSe})$  as vapors and solids and in various solvents. The  $\nu(\text{CO})$  region of the normal selenocarbonyl derivative has also been investigated at 15 K. Definitive assignments are proposed for most of the fundamental vibrations of these molecules as well as for the related species  $\text{W}(\text{CO})_5(\text{CS})$  and *trans*- $\text{W}(\text{CO})_4(\text{CSe})$ , on the basis of general quadratic valence potential fields employing both compliance and force constants. The  $\nu(\text{CO})$  and  $\nu(\text{CX})$  modes in these calculations were corrected for anharmonicity. The  $\sigma$ -donor/ $\pi$ -acceptor capacities of the chalcocarbonyl ligands are discussed in terms of the interaction displacement coordinates which were derived from the MC and CX compliance constants. The vibrational results reported provide further evidence for the transferability of compliance and force constants between species of closely related geometry and also for the similar bonding properties of the CS and CSe ligands.

### Introduction

The recent discovery of the simple selenocarbonyl complex  $\text{Cr}(\text{CO})_5(\text{CSe})$ <sup>1</sup> presents the best opportunity to date to study the relative bonding capabilities of the three isoelectronic ligands CO, CS, and CSe in structurally related metal carbonyl complexes. The  $\text{Cr}(\text{CO})_5(\text{CX})$  ( $\text{X} = \text{O}, \text{S}, \text{Se}$ ) series is particularly suitable for a comparative vibrational study since the potential constants of  $\text{Cr}(\text{CO})_6$  are already well established.<sup>2</sup> Furthermore, because of the structural similarities of the complexes, most of the potential constants not involving the heteroligand should remain essentially unchanged.

In order to have sufficient vibrational data to produce reliable potential fields for the pentacarbonylchromium(0) chalcocarbonyl complexes, we prepared the all-<sup>13</sup>C- and mono-<sup>13</sup>C-labeled derivatives, and their spectra were analyzed. The anharmonicity corrections determined previously for the CO, CS, and CSe stretching modes<sup>3</sup> were employed to calculate harmonic frequencies, and the normal mode calculations were performed with use of compliance constants rather than the more familiar force constants for the reasons explained in detail by Jones.<sup>4</sup> A compliant field was also

(1) A. M. English, K. R. Plowman, I. S. Butler, G. Jaouen, P. LeMaux, and J.-Y. Thepot, *J. Organomet. Chem.*, **132**, C1 (1977).

(2) L. H. Jones, R. S. McDowell, and M. Goldblatt, *Inorg. Chem.*, **8**, 2349 (1969).

(3) (a) A. M. English, Ph.D. Thesis, McGill University, Montreal, Canada, 1980; (b) A. M. English, J. Sedman, K. R. Plowman, and I. S. Butler, submitted for publication in *J. Mol. Spectrosc.*

(4) L. H. Jones, "Inorganic Vibrational Spectroscopy", Marcel Dekker, New York, 1971.

determined for  $W(CO)_5(CS)$  with use of the vibrational data reported previously for this complex and its *trans*-mono- $^{13}CO$  derivative.<sup>5</sup> It should be mentioned, however, that although compliance constants were used in the calculations, the final potential fields are expressed in both force and compliance constants. Valence force fields had already been obtained in this laboratory for  $Cr(CO)_5(CS)$  and  $W(CO)_5(CS)$ ,<sup>5</sup> but the wavenumber fit of many of the observed bands was not totally satisfactory—the only additional isotopic species examined was *trans*- $W(CO)_4(^{13}CO)(CS)$  which supplied relatively few extra data for the vibrational analysis—and the  $\nu(CO)$  and  $\nu(CS)$  modes were not corrected for anharmonicity. Furthermore, the use of force rather than compliance constants prevented the direct transfer of the angle bending constants from  $M(CO)_6$  to  $M(CO)_5(CS)$  due to the redundancy in the CMC coordinates.

In this paper, we present the results of these detailed normal coordinate calculations. The interactions among the MC and CX bond stretches are interpreted with use of interaction coordinates. These latter quantities are readily derived from the compliant constants,<sup>4</sup> and a comparison of the values obtained for these quantities with the results of MO calculations on  $Cr(CO)_6$  and  $Cr(CO)_5(CS)$ <sup>6</sup> leads to a consistent description of bonding of the heteroligands.

### Experimental Section

The  $Cr(CO)_5(CX)$  complexes were prepared as described earlier<sup>1</sup> and were sublimed immediately prior to use. All IR spectra in the 4000–200- $cm^{-1}$  region were recorded on a Perkin-Elmer Model 521 grating spectrophotometer. The bands were calibrated against the vibrational-rotational spectra of gaseous CO,  $NH_3$ , and HCl and water vapor<sup>7</sup> (accuracy  $\pm 0.5\text{ cm}^{-1}$ ). Gas-phase IR spectra were obtained with use of a 10-cm gas cell fitted with CsI windows, and the  $CS_2$ ,  $CH_2Cl_2$ , and  $CCl_4$  solution spectra were obtained with use of matched 0.1- and 0.2-mm KBr solution cells. The Raman spectra of the powdered solids and  $CH_2Cl_2$  solutions (in sealed Pyrex capillaries) were recorded on a Jarrell-Ash Model 25-300 Raman spectrometer with use of the yellow 568.1-nm line of a Coherent Radiation krypton-ion laser (Model 52K) for excitation. The laser power at the samples was ca. 50–100 mW for the solids and 50 mW or less for the solutions. No decomposition of the thiocarbonyl solutions was evident during the period of observation, while rapid decomposition of the selenocarbonyl solutions prevented recording of peaks other than the most intense ones. Low-temperature data were obtained with use of a closed-cycle helium cryogenic unit (Cryodyne Cryocooler, Model 21, Cryogenic Technology Inc., Waltham, Mass.). All the Raman spectra were calibrated against the emission lines of a standard neon lamp, and the band positions are generally accurate to  $\pm 0.5\text{ cm}^{-1}$ . The spectral resolution employed was usually in the 1–2- $cm^{-1}$  range.

### Results and Discussion

As mentioned in the Introduction, the vibrational spectra of  $Cr(CO)_5(CS)$ ,  $W(CO)_5(CS)$ , and the mono- $^{13}CO$ -substituted derivative *trans*- $W(CO)_4(^{13}CO)(CS)$  (90%  $^{13}C$  enriched) have been analyzed previously in this laboratory.<sup>5</sup> Assignments were proposed for the fundamental modes largely on the basis of the frequencies calculated with use of valence force fields transferred from the corresponding metal hexacarbonyls. The assignments in all cases were consistent with  $C_{4v}$  molecular symmetry. However, as will be shown later, a reexamination of the vibrational spectra of  $Cr(CO)_5(CS)$ , together with data from the isotopically labeled species  $Cr(^{13}CO)_5(CS)$  and  $Cr(CO)_5(^{13}CS)$ , leads to some changes in the original assignments, especially in the 700–250- $cm^{-1}$  region. The complete vibrational spectra of  $Cr(CO)_5(CSe)$  and  $Cr(^{13}CO)_5(CSe)$  are reported here for the first time. In the case of the

Vibration Type	$M(CO)_6$		$M(CO)_5(CX)$	
	Vib. No.	Sym	Sym	Vib. No.
$\nu(CO)$	$\nu_1$	$a_{1g}$	$3a_1$	$\nu_1$
	$\nu_3$	$e_g$	$b_1$	$\nu_2$
	$\nu_6$	$t_{1u}$	$e$	$\nu_3$
$\nu(MC)$	$\nu_2$	$a_{1g}$	$3a_1$	$\nu_5$
	$\nu_4$	$e_g$	$b_1$	$\nu_6$
	$\nu_8$	$t_{1u}$	$e$	$\nu_7$
$\delta(MCO)$	$\nu_5$	$t_{1g}$	$a_1$	$\nu_4$
	$\nu_7$	$t_{1u}$	$a_2$	$\nu_9$
	$\nu_{10}$	$t_{2g}$	$b_1$	$\nu_{11}$
	$\nu_{12}$	$t_{2u}$	$b_2$	$\nu_{14}$
$\delta(CMC)$	$\nu_9$	$t_{1u}$	$4e$	$\nu_{17}$
	$\nu_{11}$	$t_{2g}$		$\nu_{18}$
	$\nu_{13}$	$t_{2u}$		$\nu_{19}$
				$\nu_{21}$
$\delta(CMC)$	$\nu_9$	$t_{1u}$	$a_1$	$\nu_8$
	$\nu_{11}$	$t_{2g}$	$b_1$	$\nu_{13}$
	$\nu_{13}$	$t_{2u}$	$b_2$	$\nu_{15}$
			$\nu_{22}$	
			$\nu_{23}$	
			$\nu_{24}$	

Figure 1. Correlation diagram between  $M(CO)_6$  ( $O_h$  symmetry) and  $M(CO)_5(CX)$  ( $C_{4v}$  symmetry).

tungsten compounds, the previous assignments<sup>5</sup> were used in the compliance field calculations since no additional vibrational data were available. A detailed discussion of the assignments for the chromium chalcocarbonyls and their  $^{13}C$ -labeled derivatives is presented in the following sections. Typical spectra of the  $M(CO)_5(CX)$  derivatives were given earlier in ref 5.

**Assignment of the CO and CS (X = S, Se) Stretching Regions.** The bands observed in the CO and CX stretching regions of the IR and Raman spectra of  $Cr(CO)_5(CX)$ ,  $Cr(^{13}CO)_5(CX)$ ,  $Cr(CO)_5(^{13}CS)$ ,  $W(CO)_5(CS)$ , and *trans*- $W(CO)_4(^{13}CO)(CS)$  are listed in Table I. From the correlation diagram given in Figure 1, three IR-active ( $2a_1 + e$ ) and four Raman-active ( $2a_1 + b_1 + e$ ) modes are expected in the CO stretching region under the  $C_{4v}$  symmetry of the  $M(CO)_5(CX)$  molecules. The IR gas-phase and solution spectra are readily assigned on this basis, and the assignments given previously for the thiocarbonyl complexes (see ref 5 and references therein) are adopted here. The CO stretching region of  $Cr(CO)_5(CSe)$  is similar to that observed for  $Cr(CO)_5(CS)$ , and so the assignments for the selenocarbonyl complex follow directly from those for the thiocarbonyl complex. The weaker peaks due to partially labeled species which appear in the IR gas-phase spectra of the enriched species were assigned by means of energy-factored force fields.

Assignment of the Raman spectra in the CO region is not so straightforward. For example, reexamination of the  $CH_2Cl_2$  solution spectrum of  $Cr(CO)_5(CS)$  reveals a strongly polarized band at 2092  $cm^{-1}$  and a depolarized band ( $\rho \approx 0.8$ ) at 2025  $cm^{-1}$ . The results of the energy-factored calculations, which place the  $a_1$  axial ( $\nu_2$ ) and  $b_1$  ( $\nu_{10}$ ) modes about 5  $cm^{-1}$  apart in the IR spectra (supplementary Table Ia), suggest that the depolarized Raman band arises from a superposition of these two modes. If one of the component peaks is due to a totally symmetric mode, the resultant envelope should at least be weakly polarized. However, Bigorgne<sup>8</sup> has shown that if the

(5) I. S. Butler, A. Garcia-Rodriguez, K. R. Plowman, and C. F. Shaw III, *Inorg. Chem.*, **15**, 2602 (1976).

(6) D. L. Lichtenberger and R. F. Fenske, *Inorg. Chem.*, **15**, 2015 (1976).

(7) IUPAC Commission on Molecular Structure and Spectroscopy, "Tables of Wavenumbers for the Calibration of Infrared Spectrometers", Butterworths, London, 1961.

Table I. Observed Fundamental Modes (cm<sup>-1</sup>) for M(CO)<sub>5</sub>(CX) in the CO and CX Stretching Regions

vib no. and sym	Cr(CO) <sub>5</sub> (CS)	Cr( <sup>13</sup> CO) <sub>5</sub> (CS)	Cr(CO) <sub>5</sub> ( <sup>13</sup> CS)	Cr(CO) <sub>5</sub> (CSe)	Cr( <sup>13</sup> CO) <sub>5</sub> (CSe)	W(CO) <sub>5</sub> (CS) <sup>a</sup>	<i>trans</i> -W(CO) <sub>5</sub> - ( <sup>13</sup> CO)(CS)
IR Gas Phase							
$\nu_1, a_1$	2097.5 ms	2049.9 ms	2097.2 ms	2097.8 ms	2050.3 ms	2102 ms	2102 ms
$\nu_2, a_1$	2032.7 s	1987.5 s	2032.9 s	2037.8 s	1991.7 s	2017 s	1979 s
$\nu_{16}, e$	2007.6 vs	1964.0 vs	2008.2 vs	2010.5 vs	1965.5 vs	2002 vs	2006 vs
$\nu_3, a_1$	1279.7 s	1279.2 s	1240.1 s	1095.4 s	1093.6 s	1286 s	1284 s
IR and Raman CH <sub>2</sub> Cl <sub>2</sub> Solution <sup>b</sup>							
$\nu_1, a_1$	2092 m (2092 p)	2044 m (2046 p)	2091 m (2093 p)	2092 m	2044 m	2099 m (2097 p)	
$\nu_2, a_1$	2021 s (2025 dp)	1975 s (1978 dp)	2020 s (2024 dp)	2028 s	1983 s	2007 s (2015 p)	
$\nu_{16}, e$	1988 vs	1944 vs	1988 vs	1992 vs	1948 vs	1994 vs	
$\nu_3, a_1$	1257 s	1257 s	1226 s	1082 s	1080 s	1272 s (1269 p)	
IR CS <sub>2</sub> Solution							
$\nu_1, a_1$	2088.4 m			2087.6 m		2095 m	
$\nu_2, a_1$	2017.3 s			2023.4 s		1965 m	
$\nu_{16}, e$	1989.0 vs			1991.8 vs		1983 s	
$\nu_3, a_1$	1261.0 s			1077.4 s		1265 s	
IR CCl <sub>4</sub> Solution							
$\nu_1, a_1$	2091 m	2091 m		2090.5 m	2042.4 m		
$\nu_2, a_1$	2022 s	2022 s		2028 s	1982 s		
$\nu_{16}, e$				1996.6 vs	1952 vs		
$\nu_3, a_1$	1266.8 s	1228.3 s		1983.4 s	1081.5 s		
Raman <sup>d</sup> Solid							
$\nu_1, a_1$	2089.0 w	2040.6 w	2089.0 w	2095.4 w 2087.8 w 2084.0 w, sh 2041.3 ms	2058.8 w 2047.5 w 2040.1 w, sh 1995.2 ms	2102 m	2091 w
$\nu_{10}, b_1$	2031 w, sh <sup>c</sup>	1986 w, sh	2032 w, sh	2028 m, sh 2023.5 s	1982.7 m, sh 1980.8 s	2025 vw	2022 vw
$\nu_2, a_1$ $\nu_{16}, e$	} 2014 m	1968 m	2014 m	2014.3 s	1970.0 s	2003 w	1954 w
				2006.0 ms	1962.0 ms		2008 mw
				1994.3 m	1951.1 m		
				1971.1 w	1929.2 w		
$\nu_3, a_1$	1266 w	1268 w	1228 w	1100 w	1098 w	1261 vw	1264 vw

<sup>a</sup> Data for tungsten complexes from ref 1. <sup>b</sup> Raman data in brackets. <sup>c</sup> sh = shoulder. <sup>d</sup> In the Raman spectrum of solid Cr(CO)<sub>5</sub>(CSe) at 15 K two additional bands are observed at 2044 and 1973 cm<sup>-1</sup>.

ratio of the amplitudes of S<sub>1</sub> to S<sub>2</sub> (equatorial and axial CO symmetry coordinates, respectively) is -1/2 in  $\nu_1$  and +1/2 in  $\nu_2$  and if the molecular polarizability derivatives with respect to the equatorial and axial CO internal coordinates are equal, a highly polarized band will be observed for  $\nu_1$  and an essentially depolarized band for  $\nu_2$ . The amplitudes of S<sub>1</sub> and S<sub>2</sub> have the above ratios if the equatorial and axial CO stretching force constants are equal.

Attempts to obtain Raman solution data for Cr(CO)<sub>5</sub>(CSe) in the  $\nu$ (CO) region failed because the complex decomposed rapidly in the laser beam. The spectra of the tungsten thiocarbonyl complex were not reinvestigated, but the Raman solution data previously reported<sup>5</sup> indicated the presence of two polarized  $\nu$ (CO) bands. This suggests that the mixing of S<sub>1</sub> and S<sub>2</sub> in the CO stretching modes is somewhat different for the chromium and tungsten thiocarbonyls. After presentation of the eigenvectors, this point will be discussed further. Unfortunately, no solution Raman data were recorded for *trans*-W(CO)<sub>5</sub>(<sup>13</sup>CO)(CS);<sup>5</sup> in this complex, the a<sub>1</sub> axial mode ( $\nu_2$ ) should be shifted considerably to lower energy, thus allowing a more precise measurement of its depolarization ratio. No peak attributable to the e  $\nu$ (CO) mode ( $\nu_{16}$ ) was observed in the Raman solution spectra of any of the complexes.

The solid-state Raman spectra in the  $\nu$ (CO) region also show some interesting features. As previously reported,<sup>5</sup> both solid Cr(CO)<sub>5</sub>(CS) and W(CO)<sub>5</sub>(CS) exhibit a broad, unsymmetric feature at ~2010 cm<sup>-1</sup> and a weak band around

2100 cm<sup>-1</sup> in their Raman spectra. The weak band can readily be assigned to the a<sub>1</sub> equatorial CO stretch ( $\nu_1$ ) by comparison with the solution and gas-phase spectra, while the second, broader peak, which possesses a shoulder on its high-energy side, is assigned to the remaining CO modes (Table I).

In contrast to the thiocarbonyl complexes, the Raman spectrum of solid Cr(CO)<sub>5</sub>(CSe) displays a multitude of bands in its  $\nu$ (CO) region (at 15 K, 12 peaks are observed). The crystal structure of Cr(CO)<sub>5</sub>(CSe) has not been determined but both Cr(CO)<sub>5</sub><sup>9</sup> and Cr(CO)<sub>5</sub>(CS)<sup>10</sup> crystallize in the centrosymmetric space group *Pnma* (*D*<sub>2h</sub><sup>6</sup>) with four molecules (on C<sub>s</sub> sites) per unit cell. If Cr(CO)<sub>5</sub>(CSe) were isostructural with Cr(CO)<sub>5</sub> and Cr(CO)<sub>5</sub>(CS), the correlation between C<sub>4v</sub> molecular symmetry, C<sub>s</sub> site symmetry, and D<sub>2h</sub> factor group symmetry would indicate that the nondegenerate modes of Cr(CO)<sub>5</sub>(CSe) could theoretically be split into two IR-active and two Raman-active components [*a*<sub>g</sub>(R) + *b*<sub>1g</sub>(R) + *b*<sub>2u</sub>(IR) + *b*<sub>3u</sub>(IR)] in the crystal. The doublet centered at ~2080 cm<sup>-1</sup> in the room-temperature Raman spectrum almost certainly corresponds to the a<sub>1</sub> equatorial  $\nu$ (CO) mode ( $\nu_1$ ) in the free molecule. Closer examination of this doublet reveals a shoulder at 2084.0 cm<sup>-1</sup> on the low-energy peak, and at 15 K three bands are clearly resolved in this region. This suggests that, unless the third peak is due to a combination mode involving

(8) M. Bigorgne, *Spectrochim. Acta, Part A*, **32A**, 1365 (1976).

(9) (a) B. Whitaker and J. W. Jeffery, *Acta Crystallogr.*, **23**, 977 (1967); (b) A. Jost, B. Rees, and W. B. Yelon, *Acta Crystallogr., Sect. B*, **B31**, 2649 (1975).

(10) J. Y. Saillard and D. Grandjean, *Acta Crystallogr., Sect. B*, **B34**, 3318 (1978).

**Table II.** Observed Fundamental Modes for  $\text{Cr}(\text{CO})_5(\text{CX})$ ,  $\text{Cr}^{13}\text{CO}_5(\text{CX})$  ( $X = \text{S}, \text{Se}$ ) and  $\text{Cr}(\text{CO})_5(^{13}\text{CS})$  in the 700–250- $\text{cm}^{-1}$  Region

vib no. and sym	$\text{Cr}(\text{CO})_5(\text{CS})$	$\text{Cr}(\text{CO})_5(^{13}\text{CS})$	$\text{Cr}^{13}\text{CO}_5(\text{CS})$	$\text{Cr}(\text{CO})_5(\text{CSe})$	$\text{Cr}^{13}\text{CO}_5(\text{CSe})$
IR Gas Phase					
$\nu_4, a_1$	650.4 s	649.6 s	639.6 s	643.1 s	631.4 s
$\nu_{17}, e$					
$\nu_{18}, e$	512 vw	510 vw	497 vw	509 vw	489 vw
$\nu_{19}, e$	488 vw	487 vw	475 vw	481 vw	472 vw
$\nu_{20}, e$	424.6 w	423.2 w	417.8 w	419.8 w	413.9 w
$\nu_5, a_1$	421.2 w	420.8 w	415.0 w	406.4 w	400.4 w
$\nu_6, a_1$	376.0 w	376.1 w	370 w	370.2 w	363.2 w
$\nu_{21}, e$	340.7 vw	335.3 vw	335.8 vw	328.3 w	323.8 vw
IR $\text{CH}_2\text{Cl}_2$ Solution					
$\nu_{17}, e$	647.2 s	646.4 s	636.4 s	639.1 s	629.2 s
$\nu_{18}, e$	513 vw	510.5 w	498.6 w	505.4 w	490 vw
$\nu_{19}, e$		485.8 w	475.4 w	480.1 w	467.6 w
$\nu_{20}, e$	430.4 m	427.4 m	424.3 m	423.1 m	416.8 m
$\nu_5, e$	422 mw	422 mw	415.7 mw	408.0 mw	399.8 w
$\nu_6, a_1$	378.4 w	377.9 w	372.7 w	372.0 w	365.4 w
$\nu_{21}, e$	340.5 vw	334.4 vw	333.3 vw		
Raman $\text{CH}_2\text{Cl}_2$ Solution					
$\nu_4, a_1$	649 p	648.4 p	634.8 p		626 p?
$\nu_{11}, b_1$	512 dp?		499 dp?		
$\nu_{19}, e$	487 dp?		475 dp?		
$\nu_5, a_1$	421 p	421.1 p	415 p	404 p	398 p
$\nu_6, a_1$	378.8 p	377.9 p	373.9 p	376.8 p	366.7 p
$\nu_7, a_1$	346.6 p	345.9 p	343.7 p	a	a
Raman Solid					
$\nu_4, a_1$	658.2 w	656.2 w	645.4 w	640.2 w	631.4 w
$\nu_{17}, e$	643.0 w	640.9 w	628.6 w	630.2 w	618.5 w
$\nu_{14}, b_2$	525 vw	524.7 vw	507.6 vw	528 vw	508 vw
$\nu_{11}, b_1$	511 w	510 w	495.6 w	505.5 w	490 w
$\nu_{19}, e$	487.6 w	484.7 w	475.0 w	480.5 w	468.4 w
$\nu_{20}, e$				425.5 w	419.4 w
$\nu_5, a_1$	423.6 ms	423.6 ms	416.9 ms	407.8 ms	401.6 ms
$\nu_6, a_1$	380.1 s	380.5 s	373.9 s	379 s	375.8 s
$\nu_7, a_1$	351.1 vs	348.2 vs	347.1 vs	280.1 vs	278.4 vs
$\nu_{21}, e$	339.5 w, sh	334 w, sh	334 w, sh	327.1 m	327.2 m

<sup>a</sup> Obscured by solvent peak.

a CO stretch and a MCO bend,  $\text{Cr}(\text{CO})_5(\text{CSe})$  may not be isostructural with  $\text{Cr}(\text{CO})_5(\text{CS})$  and  $\text{Cr}(\text{CO})_6$ . An attempt to supplement the Raman data for solid  $\text{Cr}(\text{CO})_5(\text{CSe})$  by recording its IR spectrum in a KBr disk failed because of rapid sublimation of the complex out of the disk.

The observed  $\nu(\text{CX})$  values from the IR and Raman spectra of all the complexes studied are also presented in Table I. As observed previously for the thiocarbonyl complexes,<sup>5</sup> the only prominent feature in the IR spectrum of  $\text{Cr}(\text{CO})_5(\text{CSe})$  in the 1900–700- $\text{cm}^{-1}$  region is the peak attributable to  $\nu(\text{CSe})$  at 1095.4  $\text{cm}^{-1}$ . Furthermore, the weak Raman activity found for  $\nu(\text{CS})$ <sup>5</sup> extends to  $\nu(\text{CSe})$ . On the basis of molecular orbital calculations, Lichtenberger and Fenske<sup>6</sup> have accounted for the weak Raman activity of  $\nu(\text{CS})$  in metal thiocarbonyls and similar arguments are expected to apply to  $\text{Cr}(\text{CO})_5(\text{CSe})$ .

**Assignment of the 700–40- $\text{cm}^{-1}$  Region.** This region has been assigned previously for  $\text{Cr}(\text{CO})_5(\text{CS})$ ,  $\text{W}(\text{CO})_5(\text{CS})$ , and *trans*- $\text{W}(\text{CO})_4(^{13}\text{CO})(\text{CS})$ .<sup>5</sup> The previous assignments are adopted here for the tungsten complexes since no additional data are available. In the case of the chromium thiocarbonyl complex, the extra data obtained from the spectra of the <sup>13</sup>C-labeled species  $\text{Cr}^{13}\text{CO}_5(\text{CS})$  and  $\text{Cr}(\text{CO})_5(^{13}\text{CS})$  as well as the observation of some extra bands for the parent complex lead to some changes in the assignments. Table II contains the data obtained for all the complexes in the 700–250- $\text{cm}^{-1}$  region. From the correlation diagram in Figure 1, we expect the MCO and MCX bending modes and the MC stretching modes in this region. Isotopic substitution at either the carbon or oxygen positions of the carbonyl groups allows one to distinguish between bending and stretching modes.<sup>2,11</sup> On <sup>13</sup>CO

substitution,  $\nu[\text{MC}(\text{O})]$  modes exhibit only a slight downward shift while  $\delta(\text{MCO})$  modes show a significant decrease in energy; for <sup>18</sup>O substitution, the opposite is true. The shifts observed on changing S to Se help to isolate those peaks involving the MCX ( $X = \text{S}, \text{Se}$ ) moiety.

Seven modes ( $a_1 + a_2 + b_1 + b_2 + 3e$ ) exhibiting  $\delta(\text{MCO})$  isotopic behavior are expected between 700 and 450  $\text{cm}^{-1}$  (Figure 1). The  $b_1$  and  $b_2$  modes should be only Raman active, and the  $a_2$  mode should be inactive. With the assignments of Jones et al. for  $\text{Cr}(\text{CO})_6$ ,<sup>2</sup> two bands ( $a_1 + e$ ) are expected at 660  $\text{cm}^{-1}$  in the IR and Raman spectra of  $\text{Cr}(\text{CO})_5(\text{CX})$ . However, only one band is observed in the IR vapor spectra of the complexes. The  $\text{CH}_2\text{Cl}_2$  solution spectra of the thiocarbonyl exhibit an IR and a polarized Raman band at  $\sim 2$   $\text{cm}^{-1}$  apart. Since both these modes are expected to be strong in the IR, the intense band at 650.4  $\text{cm}^{-1}$  in the IR spectrum of  $\text{Cr}(\text{CO})_5(\text{CS})$  vapor [at 643.1  $\text{cm}^{-1}$  for  $\text{Cr}(\text{CO})_5(\text{CSe})$  vapor] is assigned to both the  $a_1(\phi)_4$  and  $e(\beta)_{17}$  modes [a weak peak at 669  $\text{cm}^{-1}$  in the IR spectrum of the thiocarbonyl complex was previously assigned to the  $a_1$  mode,<sup>5</sup> but this peak is most probably due to a small amount of  $\text{Cr}(\text{CO})_6$  impurity; it appears in the spectra of both chalcocarbonyls, and its intensity, relative to the other modes, varies for different samples of the complexes].

Again from the assignments of Jones et al.<sup>2</sup> for  $\text{Cr}(\text{CO})_6$ , the four remaining  $\delta(\text{MCO})$  modes ( $b_1 + b_2 + 2e$ ) are expected around 500  $\text{cm}^{-1}$  for  $\text{Cr}(\text{CO})_5(\text{CS})$ . The Raman

(11) D. K. Ottesen, H. B. Gray, L. H. Jones, and M. Goldblatt, *Inorg. Chem.*, **12**, 1051 (1973).

Table III. Calculated and Observed Wavenumbers (cm<sup>-1</sup>) for CMC Deformation Modes

vib no. and sym	Cr(CO) <sub>5</sub> (CS)			Cr(CO) <sub>5</sub> ( <sup>13</sup> CS)			Cr( <sup>13</sup> CO) <sub>5</sub> (CS)			Cr(CO) <sub>5</sub> (CSe)			Cr( <sup>13</sup> CO) <sub>5</sub> (CSe)		
	calcd	Raman solid	IR <sup>a</sup> combn	calcd	Raman solid	IR combn	calcd	Raman solid	IR combn	calcd	Raman solid	IR combn	calcd	Raman solid	IR combn
$\nu_8, a_1$	93.8	105	98	93.6	104.5	98	93.5	104		86.4	109	86	86.2	109	
$\nu_{13}, b_1$	67.9			67.9			67.4			67.9	68		67.4	67	
$\nu_{15}, b_2$	89.4			84.4			89.1			89			89.1		
$\nu_{22}, e$	94.8	95	98	94.8	95	98	94.4	95	98	94.7		95.5	94.2		95.6
$\nu_{23}, e$	80.0			80.0			79.6			78.3			77.9		
$\nu_{24}, e$	57.0	56	56.7	57.0		56.9	56.7			48.4	45.5 <sup>b</sup>		48.0	45.2 <sup>b</sup>	

<sup>a</sup> These wavenumbers were determined from IR combination bands. 39.3 and 51.2 cm<sup>-1</sup>.

<sup>b</sup> Average values for doublets with peaks at 40.0 and 51.0 cm<sup>-1</sup> and

spectra of the solid chromium chalcocarbonyls and the IR spectra of their vapors exhibit three and two very weak peaks, respectively, in this region. All peaks show  $\delta$ (MCO) isotopic behavior, but the two IR bands are coincident with two of the Raman bands. Based on the calculated frequencies for Cr(CO)<sub>5</sub>(CS),<sup>5</sup> the 488-cm<sup>-1</sup> peak in the IR and Raman spectra of this complex is assigned to an e  $\delta$ (MCO) mode, and the Raman band at 525 cm<sup>-1</sup> is assigned to b<sub>2</sub>( $\beta$ )  $\nu_{14}$ . The two remaining MCO modes of e and b<sub>1</sub>( $\phi$ )  $\nu_{11}$  symmetries are assigned to the 512-cm<sup>-1</sup> band in the IR and Raman spectra, respectively. This latter assignment is strengthened by the fact that the inactive t<sub>1u</sub> mode of Cr(CO)<sub>6</sub>, which gives rise to b<sub>1</sub> + e modes under C<sub>4v</sub>, was assigned a frequency of 510.9 cm<sup>-1</sup> from the observed combination spectra of Cr(CO)<sub>6</sub>.<sup>2</sup>

The assignments for the selenocarbonyl complex follow from the thiocarbonyl. The e  $\delta$ (MCX) mode ( $\nu_{21}$ ) is attributed to the weak peaks at 340.7 and 328.3 cm<sup>-1</sup> in the IR vapor-phase spectra of the thiocarbonyl and selenocarbonyl complexes, respectively, largely because of the mass effect observed on replacing S by Se.

Assignment of the  $\nu$ (MC) modes is somewhat simplified by their characteristic Raman intensity in addition to their isotopic behavior. The three intense bands observed in the Raman spectra of solid Cr(CO)<sub>5</sub>(CS) (at 423.6, 380.1, and 351.1 cm<sup>-1</sup>) and solid Cr(CO)<sub>5</sub>(CSe) (at 407.8, 379.0, and 280.1 cm<sup>-1</sup>) are assigned to the three a<sub>1</sub>  $\nu$ (MC) modes. The shifts observed in the first and third peaks on changing S to Se suggest that these be assigned to the a<sub>1</sub> axial  $\nu$ [MC(O)] ( $\nu_5$ ) and the a<sub>1</sub>  $\nu$ [MC(X)] ( $\nu_7$ ) modes, respectively. The a<sub>1</sub> equatorial  $\nu$ [MC(O)] mode ( $\nu_6$ ) is expected to be the least perturbed on substitution of an axial ligand and is, therefore, assigned to the middle band. The Raman spectrum of solid Cr(CO)<sub>5</sub>(C-Se) shows a fourth, weaker band at 425.5 cm<sup>-1</sup> which is assigned to the e equatorial  $\nu$ [MC(O)] mode ( $\nu_{20}$ ); in the thiocarbonyl complex, this mode is apparently buried beneath the intense a<sub>1</sub> mode ( $\nu_5$ ). However, in the IR solution spectrum (CH<sub>2</sub>Cl<sub>2</sub>) of Cr(CO)<sub>5</sub>(CS),  $\nu_5$ (a<sub>1</sub>) and  $\nu_{20}$ (e) appear as a poorly resolved doublet. The lower-energy component of this doublet is coincident with a polarized Raman band and so is assigned to  $\nu_5$ (a<sub>1</sub>).

The previously calculated wavenumbers for Cr(CO)<sub>5</sub>(CS)<sup>5</sup> predict that the b<sub>1</sub>  $\nu$ [MC(O)] mode ( $\nu_{12}$ ) should occur at 390 cm<sup>-1</sup>, yet no band was observed in the Raman spectrum at this position. Assignment of this mode is based, instead, on a binary combination observed in the CS<sub>2</sub> solution IR spectra of Cr(CO)<sub>5</sub>(CS) and Cr(CO)<sub>5</sub>(CSe) at 2379 and 2381 cm<sup>-1</sup>, respectively. Attributing these peaks to binary combinations of the e  $\nu$ (CO) mode ( $\nu_{16}$ ) and  $\nu_{12}$  predicts values of 390 and 389 cm<sup>-1</sup> for the latter. The previous assignment of the first overtone of the inactive a<sub>2</sub>  $\delta$ (MCO) mode ( $\nu_9$ ) to a peak at 728 cm<sup>-1</sup> in the solid-state Raman spectrum of Cr(CO)<sub>5</sub>(CS)<sup>5</sup> is substantiated by the observation of a corresponding peak in the spectrum of Cr(<sup>13</sup>CO)<sub>5</sub>(CS) at 706.5 cm<sup>-1</sup>, thus yielding fundamentals possessing the isotopic behavior characteristic of  $\delta$ (MCO) modes. Cr(CO)<sub>5</sub>(CSe) and Cr(<sup>13</sup>CO)<sub>5</sub>(CSe) ex-

hibit analogous peaks for 2 $\nu_9$ : 726 and 704 cm<sup>-1</sup>, respectively.

Correlation with M(CO)<sub>6</sub> (Figure 1) reveals that six (a<sub>1</sub> + b<sub>1</sub> + b<sub>2</sub> + 3 e) CMC deformation modes are expected for the M(CO)<sub>5</sub>(CX) molecules. The wavenumbers calculated for these modes using the Cr(CO)<sub>6</sub> compliant field<sup>12</sup> are given in Table III together with the observed values. The lack of vapor-phase data necessitates the use of data from solid-state Raman and IR combination spectra,<sup>3</sup> and the assignments are based on the calculated frequencies, which as Table III shows, are in good agreement.

**Calculation of Potential Constants.** The G matrix<sup>13</sup> elements were determined with use of the MC and CO lengths used by Jones et al.<sup>2</sup> for Cr(CO)<sub>6</sub> and W(CO)<sub>6</sub> with one exception. The value reported for CO in Cr(CO)<sub>6</sub> is 1.171 Å.<sup>9a</sup> However, if this value is used to calculate the G matrix element for the t<sub>1g</sub> frequency the corresponding force constant (obtained for all three isotopic species) does not agree with the published, the calculated and published values being 0.384 and 0.375 ± 0.0001 m dyn Å<sup>-1</sup>, respectively. A more recent study<sup>9b</sup> reports a CO bond length of 1.141 Å in Cr(CO)<sub>6</sub> (both values were corrected for thermal motion). If the average of these two values, 1.156 Å, and the MC value reported by Jones et al.<sup>2</sup> are used to calculate the G matrix element, the force constant calculated from all three frequencies observed for the t<sub>1g</sub> mode equals 0.377 m dyn Å<sup>-1</sup>. Furthermore, use of this average CO bond length and Jones' published compliant field<sup>12</sup> gives a better fit to the observed frequencies than that obtained with use of a CO bond length of 1.171 Å.

Bond lengths for the CS and MC(X) bonds in M(CO)<sub>5</sub>(CX) were estimated by multiplying the corresponding hexacarbonyl CO and MC bonds by the CX/CO and MC(X)/MC(O) ratios found in ( $\eta^6$ -CH<sub>3</sub>CO<sub>2</sub>C<sub>6</sub>H<sub>5</sub>)Cr(CO)<sub>2</sub>(CX) (X = O, S, Se).<sup>14</sup> The actual bond lengths input into the calculations were as follows: for Cr(CO)<sub>5</sub>(CX), CO = 1.156, CS = 1.565, CSe = 1.736, CrC(O) = 1.916, CrC(S) = 1.854, CrC(Se) = 1.835; for W(CO)<sub>5</sub>(CS), CO = 1.148, CS = 1.556, WC(O) = 2.059, WC(S) = 1.996 Å. The atomic masses used were those of the most abundant isotopes based on <sup>12</sup>C = 12.00000, viz., O = 15.99491, S = 31.07207, Cr = 83.76, and Se = 79.9165.

The internal and symmetry coordinates are the same as those previously published<sup>5</sup> and are shown here in Figure 2 and Table IV, respectively. A correction is made in Table IV to the  $\beta$  coordinate in the E block (S<sub>17a</sub>) given in ref 5. The generating coordinate used ( $\beta_2 + \beta_3$ ) is not "properly oriented" for the E<sub>a</sub> block because it is not invariant under the same symmetry operations as the other generating coordinates in this block.<sup>13</sup> The correct generating coordinate is  $\beta_2 - \beta_3$ .

(12) L. H. Jones, *J. Mol. Spectrosc.*, **36**, 398 (1970).

(13) E. B. Wilson, J. C. Decius, and P. C. Cross "Molecular Vibrations", McGraw-Hill, New York, 1955.

(14) (a) J. Y. Saillard and D. Grandjean, *Acta Crystallogr., Sect. B*, **B32**, 2285 (1976); (b) J. Y. Saillard, G. Le Borgne, and D. Grandjean, *J. Organomet. Chem.*, **94**, 409 (1975); (c) J. Y. Saillard and D. Grandjean, *Acta Crystallogr., Sect. B*, **B34**, 3772 (1978).

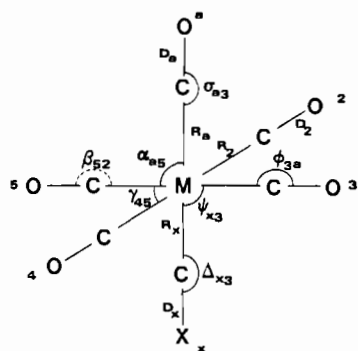


Figure 2. Internal coordinates of the  $M(CO)_5(CX)$  molecules.

Table IV. Symmetry Coordinates for the  $M(CO)_5(CX)$  Molecules<sup>a</sup>

A <sub>1</sub> Block	
$S_1 = 1/2(D_2 + D_3 + D_4 + D_5)$	$S_5 = R_a$
$S_2 = D_a$	$S_6 = 1/2(R_2 + R_3 + R_4 + R_5)$
$S_3 = D_x$	$S_7 = R_x$
$S_4 = 1/2(\phi_{2a} + \phi_{3a} + \phi_{4a} + \phi_{5a})$	$S_8 = 1/2(2^{1/2})(\alpha_{a2} + \alpha_{a3} + \alpha_{a4} + \alpha_{a5} - \psi_{x2} - \psi_{x3} - \psi_{x4} - \psi_{x5})$
A <sub>2</sub> Block	
$S_9 = 1/2(\beta_{23} + \beta_{34} + \beta_{45} + \beta_{52})$	
B <sub>1</sub> Block	
$S_{10} = 1/2(D_2 - D_3 + D_4 - D_5)$	$S_{12} = 1/2(R_2 - R_3 + R_4 - R_5)$
$S_{11} = 1/2(\phi_{2a} - \phi_{3a} + \phi_{4a} - \phi_{5a})$	$S_{13} = 1/2(2^{1/2})(\alpha_{a2} - \alpha_{a3} + \alpha_{a4} - \alpha_{a5} - \psi_{x2} + \psi_{x3} - \psi_{x4} + \psi_{x5})$
B <sub>2</sub> Block	
$S_{14} = 1/2(\beta_{23} - \beta_{34} + \beta_{45} - \beta_{52})$	
E <sub>a</sub> Block	
$S_{16a} = 1/2(D_2 + D_3 - D_4 - D_5)$	$S_{21a} = 1/2(2^{1/2})(\Delta_{x2} + \Delta_{x3})$
$S_{17a} = 1/2(\beta_{23} - \beta_{34} - \beta_{45} + \beta_{52})$	$S_{22a} = 1/2(\alpha_{a2} + \alpha_{a3} - \alpha_{a4} - \alpha_{a5})$
$S_{18a} = 1/2(\phi_{2a} + \phi_{3a} - \phi_{4a} - \phi_{5a})$	$S_{23a} = 1/2(2^{1/2})(\gamma_{23} - \gamma_{45})$
$S_{19a} = 1/2(R_2 + R_3 - R_4 - R_5)$	$S_{24a} = 1/2(\psi_{x2} + \psi_{x3} - \psi_{x4} - \psi_{x5})$
$S_{20a} = 1/2(2^{1/2})(\alpha_{a2} + \alpha_{a3})$	

<sup>a</sup> The internal coordinates and numbering of atoms are shown in Figure 2.

The symmetry compliant matrix elements were determined by the method described in ref 13 and are presented in Table V. The valence compliant labeling used here corresponds to that given for the internal coordinates in Figure 2. The superscripts c and t denote cis and trans interactions of the equatorial coordinates, respectively. The initial values for the symmetry compliants were calculated from the corresponding  $M(CO)_6$  values<sup>12</sup> and the matrix elements listed in Table V; these initial estimates are given in Table VI. The observed frequencies input to the calculation are collected in Table VII. Harmonic, vapor-phase frequencies<sup>3</sup> were used in all cases for the  $\nu(CO)$  and  $\nu(CX)$  modes, and vapor-phase data, when available, were used for the remaining frequencies.

The potential constant calculations were carried out with use of two computer programs, GMAT<sup>15</sup> and COMPLY,<sup>16</sup> which were modified for use on the McGill University IBM 360/75 computer. In the least-squares refinement of the compliance constants performed by COMPLY, the relative weighting of the frequencies is given by  $\nu_i^6/(\sigma\nu_i)^2$ , where  $\sigma\nu_i$  is the standard deviation of  $\nu_i$ . The weighting scheme used here was simply  $\nu_i^6$  as the  $\sigma\nu_i$  were considered to be unity. However, certain

Table V. Symmetry Compliants for the  $M(CO)_5(CX)$  Molecules

A <sub>1</sub> Block <sup>a</sup>	
$C_{1,1} = C_D + 2C_{DD}^c + C_{DD}^t$	$C_{2,6} = 2C_{RD}a$
$C_{2,2} = C_{D_a}$	$C_{2,7} = C_{R_x}D_a$
$C_{3,3} = C_{D_x}$	$C_{2,8} = 2^{1/2}(C_{D_a}\alpha - C_{D_a}\psi)$
$C_{4,4} = C_\phi + 2C_{\phi\phi}^c + C_{\phi\phi}^t$	$C_{3,4} = 2C_{D_x}\phi$
$C_{5,5} = C_{R_a}$	$C_{3,5} = C_{R_a}D_x$
$C_{6,6} = C_R + 2C_{RR}^c + C_{RR}^t$	$C_{3,6} = 2C_{RD_x}$
$C_{7,7} = C_{R_x}$	$C_{3,7} = C_{R_x}D_x$
$C_{8,8} = C_\alpha + 2C_{\alpha\alpha}^c + C_{\alpha\alpha}^t - C_{\alpha\psi} - 2C_{\alpha\psi}^c - C_{\alpha\psi}^t$	$C_{3,8} = 2^{1/2}(C_{D_x}\alpha - C_{D_x}\psi)$
$C_{1,2} = 2C_{DD}a$	$C_{4,5} = 2C_{R_a}\phi$
$C_{1,3} = 2C_{DD}x$	$C_{4,6} = C_{R\phi} + 2C_{R\phi}^c + C_{R\phi}^t$
$C_{1,4} = C_{D\phi} + 2C_{D\phi}^c + C_{D\phi}^t$	$C_{4,7} = 2C_{R_x}\phi$
$C_{1,5} = 2C_{R_a}D$	$C_{4,8} = 1/2(2^{1/2})(C_{\phi\alpha} + 2C_{\phi\alpha}^c + C_{\phi\alpha}^t - C_{\phi\psi} - 2C_{\phi\psi}^c - C_{\phi\psi}^t)$
$C_{1,6} = C_{RD} + 2C_{RD}^c + C_{RD}^t$	$C_{5,6} = 2C_{R_a}R$
$C_{1,7} = 2C_{R_x}D$	$C_{5,7} = C_{R_a}R_x$
$C_{1,8} = 1/2(2^{1/2})(C_{D\alpha} + 2C_{D\alpha}^c + C_{D\alpha}^t - C_{D\psi} - 2C_{D\psi}^c - C_{D\psi}^t)$	$C_{5,8} = 2^{1/2}(C_{R_a}\alpha - C_{R_a}\psi)$
$C_{2,3} = C_{D_a}D_x$	$C_{6,7} = 2C_{RR_x}$
$C_{2,4} = 2C_{D_a}\phi$	$C_{6,8} = 1/2(2^{1/2})(C_{R\alpha} + 2C_{R\alpha}^c + C_{R\alpha}^t - C_{R\psi} - 2C_{R\psi}^c - C_{R\psi}^t)$
$C_{2,5} = C_{R_a}D_a$	$C_{7,8} = 2^{1/2}(C_{R_x}\alpha - C_{R_x}\psi)$
A <sub>2</sub> Block	
$C_{9,9} = C_\beta + 2C_{\beta\beta}^c + C_{\beta\beta}^t$	
B <sub>1</sub> Block	
$C_{10,10} = C_D - 2C_{DD}^c + C_{DD}^t$	$C_{10,12} = C_{RD} - 2C_{RD}^c + C_{RD}^t$
$C_{11,11} = C_\phi - 2C_{\phi\phi}^c + C_{\phi\phi}^t$	$C_{10,13} = 1/2(2^{1/2})(C_{D\alpha} - 2C_{D\alpha}^c + C_{D\alpha}^t - C_{D\psi} + 2C_{D\psi}^c - C_{D\psi}^t)$
$C_{12,12} = C_R - 2C_{RR}^c + C_{RR}^t$	$C_{11,12} = C_{R\phi} - 2C_{R\phi}^c + C_{R\phi}^t$
$C_{13,13} = C_\alpha - 2C_{\alpha\alpha}^c + C_{\alpha\alpha}^t - C_{\alpha\psi} + 2C_{\alpha\psi}^c - C_{\alpha\psi}^t$	$C_{11,13} = 1/2(2^{1/2})(C_{\phi\alpha} - 2C_{\phi\alpha}^c + C_{\phi\alpha}^t - C_{\phi\psi} + 2C_{\phi\psi}^c - C_{\phi\psi}^t)$
$C_{10,11} = C_{D\phi} - 2C_{D\phi}^c + C_{D\phi}^t$	$C_{12,13} = 1/2(2^{1/2})(C_{R\alpha} - 2C_{R\alpha}^c + C_{R\alpha}^t - C_{R\psi} + 2C_{R\psi}^c - C_{R\psi}^t)$
B <sub>2</sub> Block	
$C_{14,14} = C_\beta - 2C_{\beta\beta}^c + C_{\beta\beta}^t$	
$C_{15,15} = C_\gamma - 2C_{\gamma\gamma}^c + C_{\gamma\gamma}^t$	
E Block	
$C_{16,16} = C_D - C_{DD}^t$	$C_{17,24} = 2C_{\beta\psi}^c$
$C_{17,17} = C_\beta - C_{\beta\beta}^t$	$C_{18,19} = C_{R\phi} - C_{R\phi}^t$
$C_{18,18} = C_\phi - C_{\phi\phi}^t$	$C_{18,20} = 2^{1/2}C_{\phi\sigma}$
$C_{19,19} = C_R - C_{RR}^t$	$C_{18,21} = 2^{1/2}C_{\phi\Delta}$
$C_{20,20} = C_\sigma$	$C_{18,22} = C_{\phi\alpha} - C_{\phi\alpha}^t$
$C_{21,21} = C_\Delta$	$C_{18,23} = 2^{1/2}(C_{\phi\gamma} - C_{\phi\gamma}^t)$
$C_{22,22} = C_\alpha - C_{\alpha\alpha}^t$	$C_{18,24} = C_{\phi\psi} - C_{\phi\psi}^t$
$C_{23,23} = C_\gamma - C_{\gamma\gamma}^t$	$C_{19,20} = 2^{1/2}C_{R\sigma}$
$C_{24,24} = C_\psi - C_{\psi\psi}^t$	$C_{19,21} = 2^{1/2}C_{R\Delta}$
$C_{16,17} = C_{D\beta} + 2C_{D\beta}^c - C_{D\beta}^t$	$C_{19,22} = C_{R\alpha} - C_{R\alpha}^t$
$C_{16,18} = C_{D\phi} - C_{D\phi}^t$	$C_{19,23} = 2^{1/2}(C_{R\gamma} - C_{R\gamma}^t)$
$C_{16,19} = C_{RD} - C_{RD}^t$	$C_{19,24} = C_{R\psi} - C_{R\psi}^t$
$C_{16,20} = 2^{1/2}C_{D\sigma}$	$C_{20,21} = C_{\sigma\Delta}$
$C_{16,21} = 2^{1/2}C_{D\Delta}$	$C_{20,22} = 2^{1/2}C_{\sigma\alpha}$
$C_{16,22} = C_{D\alpha} - C_{D\alpha}^t$	$C_{20,23} = 2C_{\sigma\gamma}$
$C_{16,23} = 2^{1/2}(C_{D\gamma} - C_{D\gamma}^t)$	$C_{20,24} = 2^{1/2}C_{\sigma\psi}$
$C_{16,24} = C_{D\psi} - C_{D\psi}^t$	$C_{21,22} = 2^{1/2}C_{\Delta\alpha}$
$C_{17,18} = C_{\beta\phi} - C_{\beta\phi}^t$	$C_{21,23} = 2C_{\Delta\gamma}$
$C_{17,19} = C_{R\beta} + 2C_{R\beta}^c - C_{R\beta}^t$	$C_{21,24} = 2^{1/2}C_{\Delta\psi}$
$C_{17,20} = 2^{1/2}C_{\beta\sigma}$	$C_{22,23} = 2^{1/2}(C_{\alpha\gamma}^t - C_{\alpha\gamma})$
$C_{17,21} = 2^{1/2}C_{\beta\Delta}$	$C_{22,24} = C_{\alpha\psi} - C_{\alpha\psi}^t$
$C_{17,22} = 2C_{\beta\alpha}^c$	$C_{23,24} = 2^{1/2}(C_{\gamma\psi} - C_{\gamma\psi}^t)$
$C_{17,23} = 2^{1/2}(C_{\gamma\beta} - C_{\gamma\beta}^c)$	

<sup>a</sup> The subscripts R, D, etc. refer to the internal coordinates shown in Figure 2; the superscripts c and t represent cis and trans interactions, respectively, of the equatorial coordinates.

(15) (a) G. Overend and J. R. Scherer, *J. Chem. Phys.*, **32**, 1289 (1960); (b) R. D. Needham, Ph.D. Thesis, University of Minnesota, Minneapolis, Minn., 1965.

(16) A detailed description of this computer program is available: R. Ottinger, Ph.D. Thesis, Oregon State University, Corvallis, Oregon, 1966.

frequencies, particularly amongst the CMC bending modes, were given zero weight by assigning them a value of zero.

Table VI. Initial Estimates of the Symmetry Compliant for the  $M(\text{CO})_5(\text{CX})$  Molecules

$C_{i,j}$ (sym)	$\text{Cr}(\text{CO})_5(\text{CX})$ (X = S, Se)	$\text{W}(\text{CO})_5(\text{CS})$	$C_{i,j}$ (sym)	$\text{Cr}(\text{CO})_5(\text{CX})$ (X = S, Se)	$\text{W}(\text{CO})_5(\text{CS})$
$C_{1,1}$ ( $A_1$ )	0.05695	0.5707	$C_{14,14}$ ( $B_2$ )	3.11	2.78
$C_{2,2}$	0.05900	0.05928	$C_{15,15}$	2.04	2.78
$C_{3,3}$	0.05900	0.05928	$C_{14,15}$	0.94	0.92
$C_{4,4}$	2.29	3.22	$C_{16,16}$ (E)	0.05951	0.05981
$C_{5,5}$	0.568	0.450	$C_{17,17}$	2.03	2.48
$C_{6,6}$	0.407	0.335	$C_{18,18}$	2.89	2.68
$C_{7,7}$	0.568	0.450	$C_{19,19}$	0.734	0.552
$C_{8,8}$	1.68	1.61	$C_{20,20}$	2.46	2.58
$C_{1,2}$	-0.00154	-0.00168	$C_{21,21}$	2.46	2.58
$C_{1,3}$	-0.00154	-0.00168	$C_{22,22}$	2.20	2.64
$C_{1,4}$	0	0	$C_{23,23}$	2.36	2.49
$C_{1,5}$	0.0025	0.0037	$C_{24,24}$	2.20	2.64
$C_{1,6}$	-0.011	-0.010	$C_{16,17}$	-0.01	-0.01
$C_{1,7}$	0.0025	0.0037	$C_{16,18}$	0	0
$C_{1,8}$	0	0	$C_{16,19}$	-0.0322	-0.03
$C_{2,3}$	-0.00051	-0.00053	$C_{16,20}$	-0.0071	-0.0071
$C_{2,4}$	-0.01	-0.01	$C_{16,21}$	-0.0071	-0.0071
$C_{2,5}$	-0.0229	-0.0221	$C_{16,22}$	-0.008	-0.008
$C_{2,6}$	0.002	0.004	$C_{16,23}$	-0.0113	-0.0113
$C_{2,7}$	0.009	0.008	$C_{16,24}$	-0.008	-0.008
$C_{2,8}$	-0.011	-0.011	$C_{17,18}$	0	0
$C_{3,4}$	0.010	-0.010	$C_{17,19}$	0.28	-0.04
$C_{3,5}$	0.009	0.008	$C_{17,20}$	0.184	0.523
$C_{3,6}$	0.0025	0.0037	$C_{17,21}$	0.184	0.523
$C_{3,7}$	-0.023	-0.022	$C_{17,22}$	0.12	0.20
$C_{3,8}$	0.011	0.011	$C_{17,23}$	0.693	1.018
$C_{4,5}$	0.28	-0.04	$C_{17,24}$	0.12	0.20
$C_{4,6}$	0	0	$C_{18,19}$	0	0
$C_{4,7}$	-0.28	0.04	$C_{18,20}$	0.156	0.071
$C_{4,8}$	0.86	1.30	$C_{18,21}$	-0.156	-0.071
$C_{5,6}$	0.005	-0.013	$C_{18,22}$	0.47	0.46
$C_{5,7}$	-0.166	-0.102	$C_{18,23}$	0	0
$C_{5,8}$	0.258	0.028	$C_{18,24}$	-0.47	-0.46
$C_{6,7}$	0.005	-0.013	$C_{19,20}$	0.198	0.028
$C_{6,8}$	0	0	$C_{19,21}$	0.198	0.028
$C_{7,8}$	-0.258	-0.028	$C_{19,22}$	0.183	0.02
$C_{9,9}$ ( $A_2$ )	2.66	2.58	$C_{19,23}$	0.258	0.028
$C_{10,10}$ ( $B_1$ )	0.06003	0.06043	$C_{19,24}$	0.182	0.02
$C_{11,11}$	1.77	1.74	$C_{20,21}$	-0.43	-0.10
$C_{12,12}$	0.397	0.361	$C_{20,22}$	0.68	0.83
$C_{13,13}$	3.04	3.37	$C_{20,23}$	0.12	0.20
$C_{10,11}$	0	0	$C_{20,24}$	0.014	0.184
$C_{10,12}$	-0.0161	-0.0176	$C_{21,22}$	0.014	0.184
$C_{10,13}$	0	0	$C_{21,23}$	0.12	0.20
$C_{11,12}$	0	0	$C_{21,24}$	0.68	0.834
$C_{11,13}$	0.523	0.735	$C_{22,23}$	-0.48	-0.62
$C_{12,13}$	0	0	$C_{22,24}$	0.16	-0.14
			$C_{23,24}$	-0.48	-0.62

**$A_1$  Symmetry Compliant.** Refinement of the primary compliant alone did not lead to a stable solution for this  $8 \times 8$  block because the two CO modes,  $\nu_1$  and  $\nu_2$ , could not be fit simultaneously with use of the input value for  $C_{1,2}$ . However, when  $C_{1,1}$ ,  $C_{2,2}$ , and  $C_{1,2}$  were refined together, the final values of these compliant varied considerably for the three complexes. Large changes in  $C_{1,1}$  from its starting value are not expected since the effect of CX should be mainly trans directed. Thus, a subsequent run, constraining  $C_{1,1}$  to its initial value and refining  $C_{2,2}$  and  $C_{1,2}$ , led to rapid convergence and a somewhat reduced value for  $C_{1,2}$  for each system. Holding  $C_{1,2}$  fixed at this new value and refining all the primaries gave values for  $C_{1,1}$  which did not deviate significantly from the initial values. Furthermore, this final compliant set gives eigenvectors for  $\nu_1$  and  $\nu_2$  in which the relative amplitudes of the two CO symmetry coordinates correspond to the amplitudes predicted on the basis of the Raman polarization of these modes (vide infra).

Constraining all off-diagonal elements (except  $C_{1,2}$ ) requires that interactions such as (CO,CX) and [CX,MC(X)] are equal to the corresponding hexacarbonyl values. At face value, these appear to be rather poor approximations and require some

justification. Even with additional data from the isotopic species, the (CO,CX) interaction constants remain ill-defined [as was observed previously for (CO,CS)<sup>5</sup>] since varying the (CO,CX) interaction compliant from its initial value to zero produces changes of less than  $1 \text{ cm}^{-1}$  in the calculated frequencies. Variation in  $C_{3,7}$ , on the other hand, gives rise to large changes in both the CX and MC(X) frequencies. From an examination of the partial correlation matrix,<sup>16</sup> it is apparent that  $C_{3,7}$  and  $C_{7,7}$  are highly correlated; thus, it is necessary to constrain one of them to a predetermined value while the other is allowed to refine. Values for  $C_{3,7}$  greater and smaller than the  $M(\text{CO})_6$  values were input to the calculations. However, any  $C_{3,7}$  values leading to either (a)  $C_{\text{MC(X)}}$  greater than the  $M(\text{CO})_6$  value or (b)  $C_{\text{MC(X)}}$  substantially smaller than the  $M(\text{CO})_6$  value can be discarded. Condition a arises because MO calculations on  $M(\text{CO})_5(\text{CS})$  reveal increased M-C interaction for CS compared to CO,<sup>6</sup> and condition b arises because of the relatively small perturbation of CX on the remainder of the molecules as indicated by both the MO calculations<sup>6</sup> as well as the small variations in the MCO equatorial and axial force constants (see below). If  $C_{\text{MC(X)}}$  varied substantially from its initial value, the CX

Table VII. Wavenumbers Input to Compliant Calculations for the  $M(\text{CO})_5(\text{CX})$  Molecules

$\nu_i$	$\text{Cr}(\text{CO})_5(\text{CS})$	$\text{Cr}(\text{CO})_5(^{13}\text{CS})$	$\text{Cr}(^{13}\text{CO})_5(\text{CS})$	$\text{Cr}(\text{CO})_5(\text{CSe})$	$\text{Cr}(^{13}\text{CO})_5(\text{CSe})$	$\text{W}(\text{CO})_5(\text{CS})^a$	$\text{W}(\text{CO})_5(^{13}\text{CO})(\text{CS})$
$\nu_1$ ( $a_1$ )	2118.1	2117.9	2069.6	2116.0	2068.0	2123	2118
$\nu_2$	2060.7	2060.8	2014.4	2064.6	2017.7	2045	2006
$\nu_3$	1287.3	1247.4	1287.0	1101.1	1099.3	1294	1292
$\nu_4$	650.4	649.6	639.6	643.1	631.4	569	
$\nu_5$	421.2	421.0	415	406.4	400.4	426	425
$\nu_6$	376.0	376.0	370	370.2	363.2	380	371
$\nu_7$	346.6	345.9	343.7	280.1	278.4	346	345
$\nu_8$	95			85		80	
$\nu_9$ ( $a_2$ )	364	364	353	363	352		
$\nu_{10}$ ( $b_1$ )	2052.4		2006.0	2054.3	2008.0	2054	2054
$\nu_{11}$	511.0	510.0	495.6	505.5	490	518	
$\nu_{12}$	390			389		412	
$\nu_{13}$				68	67		
$\nu_{14}$ ( $b_2$ )	525	526	507.6	528	508	479	
$\nu_{15}$	85			85	84		
$\nu_{16}$ ( $e$ )	2044.9	2044.8	1999.4	2044.6	1998.7	2039	2039
$\nu_{17}$	650.4	649.6	639.6	643.1	631.4	569	
$\nu_{18}$	525	526	507.6	528	508	491	483
$\nu_{19}$	487.6	484.7	475.0	480.5	468.4	463	463
$\nu_{20}$	424.6	423.2	417.8	419.8	413.9	375	
$\nu_{21}$	340.7	335.3	335.8	328.3	323.8	332	331
$\nu_{22}$	95			95			
$\nu_{23}$							
$\nu_{24}$	56			46		50	

<sup>a</sup> Data for tungsten complexes from ref 5.Table VIII. Wavenumber Errors for the Fundamental Modes of the  $M(\text{CO})_5(\text{CX})$  Molecules ( $X = \text{S}, \text{Se}$ )<sup>a,b</sup>

$\nu_i$	$\text{Cr}(\text{CO})_5(\text{CS})$	$\text{Cr}(\text{CO})_5(^{13}\text{CS})$	$\text{Cr}(^{13}\text{CO})_5(\text{CS})$	$\text{Cr}(\text{CO})_5(\text{CSe})$	$\text{Cr}(^{13}\text{CO})_5(\text{CSe})$	$\text{W}(\text{CO})_5(\text{CS})$	$\text{W}(\text{CO})_5(^{13}\text{CO})(\text{CS})$
$\nu_1$ ( $a_1$ )	-0.1	-0.2	0.6	-0.5	0.5	-0.8	0.8
$\nu_2$	-0.4	-0.3	0.4	-0.1	0.1	-0.8	0.8
$\nu_3$	0.0	0.0	-0.3	0.9	-0.9	1.0	-1.0
$\nu_4$	-0.4	-1.2	1.6	-0.8	0.9	0.0	568.9
$\nu_5$	-0.3	-0.3	0.7	-0.5	0.4	0.5	425.5
$\nu_6$	-0.1	0.0	0.0	0.4	-0.4	2.2	-2.6
$\nu_7$	-0.1	0.6	-0.4	-0.3	0.3	0.2	0.4
$\nu_8$	1.7	93.1	93.0	-1.0	85.8	0.3	79.7
$\nu_9$ ( $a_2$ )	0.0	0.0	0.0	0.0	0.0	361.6	361.6
$\nu_{10}$ ( $b_1$ )	-0.1	2052.5	1.0	-0.5	0.8	-0.2	-0.2
$\nu_{11}$	-0.1	-1.1	1.2	-0.6	0.4	0.0	518.0
$\nu_{12}$	0.0	390.0	383.5	0.0	382.6	0.0	412.0
$\nu_{13}$	67.8	67.8	67.4	0.2	-0.3	61.1	61.1
$\nu_{14}$ ( $b_2$ )	-0.6	-0.6	1.0	0.6	-0.3	-0.1	479.1
$\nu_{15}$	89.0	89.0	88.7	-4.1	88.8	81.3	81.3
$\nu_{16}$ ( $e$ )	-0.1	-0.2	0.3	0.0	0.0	0.0	0.0
$\nu_{17}$	-0.6	0.5	-0.2	0.2	-0.3	0.0	565.3
$\nu_{18}$	-0.3	-0.2	0.3	0.0	-0.2	-0.2	0.2
$\nu_{19}$	0.2	0.4	-0.5	1.0	-0.8	-0.2	0.3
$\nu_{20}$	-0.4	0.6	0.2	-0.1	0.1	0.0	374.7
$\nu_{21}$	-0.4	0.0	0.5	-1.2	1.2	-0.9	0.8
$\nu_{22}$	1.7	93.2	92.8	0.6	94.0	83.2	83.1
$\nu_{23}$	79.1	79.1	78.7	77.1	76.7	70.4	70.4
$\nu_{24}$	-0.4	56.3	56.1	-0.4	46.1	-1.1	51.0

<sup>a</sup> Error in  $\nu_i = \nu_i(\text{obsd}) - \nu_i(\text{calcd})$ . <sup>b</sup> Calculated frequencies are given for the  $\nu_i$  not input to the refinement.

ligand would be expected to cause much larger perturbations in the remainder of the molecule, which should be reflected in significant variation in the cis and trans MCO constants (as is the case for  $\text{Mn}(\text{CO})_5\text{Br}^{11}$ ). The initial or  $M(\text{CO})_6$  values for  $C_{3,7}$  give results consistent with these conditions and are, therefore, believed to be *reasonably* good estimates of the true values. Finally, the excellent agreement between the observed and calculated frequencies (Table VIII) lends further support to the chosen fields.

**$A_2$ ,  $B_1$ , and  $B_2$  Symmetry Compliant.** Values of 2.66 and 2.68  $\text{\AA} \text{mdyn}^{-1}$  were calculated for the  $\text{Cr}(\text{CO})_5(\text{CS})$  and  $\text{Cr}(\text{CO})_5(\text{CSe})$   $A_2$  compliant, respectively, from the first overtone of the  $a_2$  mode ( $\nu_9$ ) observed in the Raman spectra of the solids. These values are equivalent to the initial value of 2.66  $\text{\AA} \text{mdyn}^{-1}$ . No Raman overtone was reported for  $\nu_9$

in the spectrum of  $\text{W}(\text{CO})_5(\text{CS})^5$ ; therefore, the final value of the  $A_2$  compliant was considered equal to the initial value of 2.58  $\text{\AA} \text{mdyn}^{-1}$ .

Rapid convergence of the  $B_1$  and  $B_2$  symmetry blocks was obtained by refining the primary constants indicated in Table IX only. This was anticipated because the initial field gave calculated frequencies almost identical with those observed for the  $b_1$  and  $b_2$  modes.

**E Symmetry Compliant.** Again, all interactions were constrained to their associated hexacarbonyl values and the field converged on refining the diagonal elements. The potential energy distributions reveal that most of the modes in this block are strongly mixed; thus, the ready convergence of such a complex problem to less than a wavenumber fit of the observed frequencies indicates that the hexacarbonyl compliant fields



**Table IX.** Final Symmetry Compliants for the  $M(\text{CO})_5(\text{CX})$  Molecules<sup>a,b</sup>

$C_{i,j}$ (sym)	$\text{Cr}(\text{CO})_5(\text{CS})$	$\text{Cr}(\text{CO})_5(\text{CSe})$	$\text{W}(\text{CO})_5(\text{CS})$
$C_{1,1}$ ( $A_1$ )	0.05694 (3) <sup>c</sup>	0.05695 (4)	0.05751 (20)
$C_{2,2}$	0.05834 (3)	0.05815 (5)	0.05911 (20)
$C_{3,3}$	0.1314 (1)	0.1746 (6)	0.1358 (6)
$C_{4,4}$	2.48 (1)	2.50 (1)	3.22 (2)
$C_{5,5}$	0.581 (2)	0.617 (2)	0.509 (6)
$C_{6,6}$	0.424 (1)	0.438 (1)	0.329 (2)
$C_{7,7}$	0.487 (2)	0.452 (3)	0.328 (5)
$C_{8,8}$	1.65 (5)	1.63 (10)	1.76 (23)
$C_{1,2}$	-0.00101 (2)	-0.00091 (3)	-0.00087 (20)
$C_{9,9}$ ( $A_2$ )	2.66	2.68	2.58
$C_{10,10}$ ( $B_1$ )	0.05960 (3)	0.05946 (2)	0.05944 (0)
$C_{11,11}$	1.77 (0)	1.81 (0)	1.75 (0)
$C_{12,12}$	0.397 (1)	0.399 (1)	0.358 (0)
$C_{13,13}$	[3.04] <sup>d</sup>	[3.04]	[3.37]
$C_{14,14}$ ( $B_2$ )	3.19 (1)	3.17 (3)	2.85 (0)
$C_{15,15}$	[2.04]	[2.04]	[2.78]
$C_{16,16}$ ( $E$ )	0.05942 (2)	0.05944 (4)	0.05974 (5)
$C_{17,17}$	1.98 (4)	2.04 (15)	2.54 (31)
$C_{18,18}$	2.67 (10)	3.10 (42)	2.64 (25)
$C_{19,19}$	0.729 (17)	0.740 (6)	0.552 (4)
$C_{20,20}$	2.80 (15)	3.08 (73)	2.96 (47)
$C_{21,21}$	2.39 (7)	1.97 (18)	2.56 (35)
$C_{22,22}$	2.44 (10)	1.93 (16)	2.31 (42)
$C_{23,23}$	2.35 (2)	2.56 (7)	2.68 (32)
$C_{24,24}$	2.32 (10)	2.63 (24)	2.66 (32)

<sup>a</sup> Units are  $\text{A mdy n}^{-1}$  for stretching compliants and  $\text{rad}^2 \text{A}^{-1} \text{mdyn}^{-1}$  for bending compliants. <sup>b</sup> All interaction compliants, except  $C_{1,2}$  ( $A_1$ ), were held fixed at the values given in Table VI. <sup>c</sup> Quantities in parentheses are the standard deviations in units of the last digit for the given compliants. <sup>d</sup> Primary compliants in square brackets were not refined.

are very good, first approximations for the present systems.

The final symmetry compliants and their standard deviations are listed in Table IX. The latter are estimates of the errors or uncertainties associated with the compliants.

**Valence Potential Constants.** The valence compliance and force constants calculated from the refined symmetry constants are given in Tables X and XI. The estimated errors in the valence compliants were obtained from those of the symmetry compliants with use of the usual relations for the propagation of errors.<sup>17</sup> No errors were calculated for some of the CMC bending compliants since the corresponding symmetry compliants were constrained in the refinements. It should be emphasized, however, that a comparison of the errors estimated for the  $M(\text{CO})_6$  and  $M(\text{CO})_5(\text{CX})$  molecules is meaningless. For example, larger errors were obtained for the  $\text{Cr}(\text{CO})_6$  compliants compared to those of  $\text{Cr}(\text{CO})_5(\text{CS})$  because the number of degrees of freedom ( $m - n$ , where  $m$  = number of observed frequencies and  $n$  = number of compliants refined<sup>16</sup>) in the refinement of the thiocarbonyl compliant field greatly exceeded that in the hexacarbonyl refinement as all off-diagonal elements were constrained in the former.

In the discussions that follow on the valence potential constants for  $M(\text{CO})_5(\text{CX})$  and their standard deviations, it should be remembered that all off-diagonal symmetry compliants (except  $C_{1,2}$ ) were held fixed. This means that only interactions within symmetry-equivalent sets of internal coordinates were refined. These valence compliants, referred to as "on-diagonal" interaction constants, appear in the expressions for the diagonal elements of the symmetry  $C$  matrix. (Likewise, the "off diagonal" elements of this matrix are linear combinations of the "off-diagonal" interaction compliants which relate to internal coordinates of different symmetry-equivalent sets.) We believe that the constraints chosen are reasonable and, therefore, impose no serious limitations on the

valence constants reported below. This allows us to draw some interesting and significant conclusions with respect to bonding in the chalcocarbonyls.

**Stretch-Stretch Constants.** From Table X, it can be seen that substitution of CX for CO in  $M(\text{CO})_6$  produces no significant difference in the equatorial CO and MC stretching constants. The main effect of CX is to reduce the axial MC(O) bond strength, as indicated by the larger axial MC(O) and the slightly smaller axial CO compliants in the chalcocarbonyls; this effect is greater in the selenocarbonyl complex than in the thiocarbonyl complex. The MC stretching constants of the substituted ligands show the reverse trend, i.e.,  $C_{\text{MC(O)}} > C_{\text{MC(S)}} > C_{\text{MC(Se)}}$ , which supports the hypothesis that MC(X)  $\pi$  back-bonding increases as X descends the chalcogens.<sup>6</sup> Also, the largely trans-directing effect of the CX ligands is similar to that noted for Br in  $\text{Mn}(\text{CO})_5\text{Br}$ .<sup>11</sup> In this complex, however,  $C_{\text{MC(axial)}} < C_{\text{MC(equatorial)}}$  since Br is a poorer  $\pi$  acceptor than CO.

In an attempt to quantify the relationship between CO stretching force constants and bonding in metal carbonyls, the Cotton-Kraihanzel force constants ( $k$ )<sup>18</sup> and the occupancies of the  $5\sigma$  and  $2\pi$  orbitals of CO (from approximate MO calculations) have been compared.<sup>19</sup> The complexes studied were a series of  $d^6$  metal carbonyl halides and dihalides of general formula  $M(\text{CO})_{6-x}\text{L}_x$  ( $M = \text{Cr, Mn, Fe; L} = \text{Cl, Br, I; } x = 1, 2$ ). The results indicate that changes in both the degree of back-bonding to the  $2\pi$  orbital and the degree of  $\sigma$  donation from the  $5\sigma$  orbital contribute to the value of  $k$ . Furthermore, a linear relationship between  $k$  and the occupancies of the  $5\sigma$  and  $2\pi$  levels was obtained:  $k = a(5\sigma) + b(2\pi_x + 2\pi_y)$ , where  $a/b = 0.405$ . Both  $a$  and  $b$  are negative, indicating that  $k$  decreases as the  $5\sigma$  and  $2\pi$  populations increase. The negative value of  $a$  is a consequence of the slightly antibonding nature of the  $5\sigma$  orbital.

One of the most obvious effects of the halogen atoms in these complexes is the preferential reduction in the force constant of the trans CO group (i.e., trans to L), e.g., in  $\text{Cr}(\text{CO})_5\text{Cl}^-$ ,  $k(\text{trans}) = 14.07$  and  $k(\text{cis}) = 15.58 \text{ mdy n } \text{\AA}^{-1}$ . This reduction is attributed to an increase in the occupancy of the  $2\pi$  levels of the trans CO, although enhanced donation from the  $5\sigma$  level opposes this effect. Since the halogen atom is essentially a  $\sigma$  donor, the difference in the cis and trans  $k$  values is due to redistribution of electron density on replacement of a CO group by a species with little or no  $\pi$ -acceptor ability.

In the thio- and selenocarbonyl complexes, on the other hand, the CO groups are replaced by ligands possessing greater  $\pi$ -acceptor ability. However, the values obtained for the cis and trans CO force constants differ by only  $0.2 \text{ mdy n } \text{\AA}^{-1}$  or less. The cis and trans CrC(O) force (and compliance) constants also show little variation, both values being similar to that of  $\text{Cr}(\text{CO})_6$  (Tables X and XI). These values are in accordance with the small differences calculated for the CrC(O) overlap populations in  $\text{Cr}(\text{CO})_5(\text{CS})$  and  $\text{Cr}(\text{CO})_6$ .<sup>6</sup> In  $\text{W}(\text{CO})_5(\text{CS})$ , a more substantial difference exists between the cis and trans WC(O) force constants, which have values of 2.41 and  $2.13 \text{ mdy n } \text{\AA}^{-1}$ , respectively. The smaller trans value can be ascribed to the increased metal-CS interaction in  $\text{W}(\text{CO})_5(\text{CS})$  as indicated by the larger WC(S) and smaller CS force constants in this complex compared to  $\text{Cr}(\text{CO})_5(\text{CS})$  (Table XI). However, the trans CO stretching force constant is not very different from the cis value or that of  $\text{W}(\text{CO})_6$ , suggesting that the reduction in  $\pi$  back-bonding is accompanied by a decrease in  $\sigma$  donation.

The "diagonal" stretch-stretch interactions, which involve the equatorial MCO groups only, do not vary significantly from their corresponding  $M(\text{CO})_6$  values. This was partly

(17) P. R. Bevington, "Data Reduction and Error Analysis for the Physical Sciences", McGraw-Hill, New York, 1969.

(18) F. A. Cotton and C. S. Kraihanzel, *J. Am. Chem. Soc.*, **84**, 4432 (1962).  
(19) M. B. Hall and R. F. Fenske, *Inorg. Chem.*, **11**, 1619 (1972).

**Table X.** Valence Compliance Constants for the  $M(\text{CO})_5(\text{CX})$  Molecules and the  $M(\text{CO})_6$  Equivalents ( $X = \text{S, Se; M} = \text{Cr, W}$ )<sup>a</sup>

$C^b$	$\text{Cr}(\text{CO})_6^{c,d}$	$\text{Cr}(\text{CO})_5(\text{CS})$	$\text{Cr}(\text{CO})_5(\text{CSe})$	$\text{W}(\text{CO})_6^c$	$\text{W}(\text{CO})_5(\text{CS})$
$C_D$	0.05900 (8)	0.05885 (1)	0.05882 (2)	0.05928 (6)	0.05911 (6)
$C_{D_a}$	0.05900 (8)	0.05834 (3)	0.05815 (5)	0.05928 (6)	0.05901 (20)
$C_{D_x}$		0.1314 (1)	0.1756 (6)		0.1358 (6)
$C_R$	0.568 (37)	0.570 (8)	0.580 (3)	0.450 (4)	0.448 (3)
$C_{R_a}$	0.568 (37)	0.581 (2)	0.617 (2)	0.450 (4)	0.509 (6)
$C_{R_x}$		0.487 (2)	0.452 (3)		0.328 (5)
$C_{DD}^c$	-0.00077 (7)	-0.00066 (1)	-0.00063 (2)	-0.00084 (3)	-0.00048 (5)
$C_{DD}^t$	-0.00051 (8)	-0.00057 (1)	-0.00062 (2)	-0.00053 (6)	-0.00063 (6)
$C_{DD_a}^c$	-0.00077 (7)	-0.00051 (1)	-0.00045 (2)	-0.00084 (4)	-0.00059 (10)
$C_{RR}^c$	0.00256 (68)	0.00674 (0)	0.00955 (0)	-0.00633 (38)	-0.00713 (0)
$C_{RR}^t$	-0.166 (37)	-0.159 (8)	-0.161 (3)	-0.102 (4)	-0.104 (3)
$C_\beta$	2.46 (33)	2.45 (2)	2.49 (8)	2.58 (20)	2.63 (16)
$C_\phi$	2.46 (33)	2.40 (5)	2.63 (21)	2.58 (20)	2.56 (12)
$C_\sigma$	2.46 (33)	2.80 (15)	3.08 (73)	2.58 (20)	2.96 (47)
$C_\Delta$		2.39 (7)	1.97 (18)		2.57 (35)
$C_{\beta\beta}^c$	-0.11 (14)	-0.13 (0)	-0.12 (0)	-0.05 (0)	-0.05 (0)
$C_{\beta\beta}^t$	0.43 (33)	0.47 (2)	0.43 (8)	0.10 (20)	0.09 (16)
$C_{\phi\phi}^c$	0.13 (30)	0.18 (0)	0.17 (0)	0.37 (10)	0.37 (0)
$C_{\phi\phi}^t$	-0.43 (33)	-0.27 (5)	-0.47 (21)	-0.10 (20)	-0.08 (12)
$C_\alpha - C_{\alpha\alpha}^t$	2.20 (41)	2.44 (10)	1.93 (16)	2.64 (25)	2.31 (42)
$C_\psi - C_{\psi\psi}^t$	2.20 (41)	2.32 (10)	2.63 (24)	2.64 (25)	2.66 (32)
$C_\gamma - C_{\gamma\gamma}^t$	2.36 (37)	2.35 (2)	2.56 (7)	2.49 (23)	2.68 (32)
$C_\alpha - C_{\alpha\psi}^c$	2.20 (41)	2.30 <sup>e</sup>	2.10 <sup>e</sup>	2.64 (25)	2.71 <sup>e</sup>
$C_{\alpha\alpha}^c - C_{\alpha\psi}^c$	-0.34 (24)	-0.34 <sup>e</sup>	-0.34 <sup>e</sup>	-0.44 (10)	-0.40 <sup>e</sup>
$C_{\alpha\alpha}^t - C_{\alpha\psi}^t$	0.16 (41)	0.16 <sup>e</sup>	0.16 <sup>e</sup>	0.14 (25)	0.13 <sup>e</sup>

<sup>a</sup> Units are given in footnote *a* of Table IX. <sup>b</sup> The subscripts and superscripts are explained in footnote *a* of Table V. <sup>c</sup>  $M(\text{CO})_6$  compliants from ref 12. <sup>d</sup> See footnote *c* of Table IX. <sup>e</sup> No errors were estimated for these constants; see text.

**Table XI.** Valence Force Constants for the  $M(\text{CO})_5(\text{CX})$  Molecules and the  $M(\text{CO})_6$  Equivalents ( $X = \text{S, Se; M} = \text{Cr, W}$ )<sup>a</sup>

$F^b$	$\text{Cr}(\text{CO})_6^c$	$\text{Cr}(\text{CO})_5(\text{CS})^d$	$\text{Cr}(\text{CO})_5(\text{CSe})$	$\text{W}(\text{CO})_6^c$	$\text{W}(\text{CO})_5(\text{CS})$
$F_D$	17.24	17.28	17.28	17.22	17.28
$F_{D_a}$	17.24	17.42	17.47	17.22	17.24
$F_{D_x}$		7.677	5.768		7.455
$F_R$	2.08	2.04	2.00	2.36	2.41
$F_{R_a}$	2.08	2.03	1.90	2.36	2.13
$F_{R_x}$		2.45	2.66		3.31
$F_{DD}^c$	0.21	0.18	0.16	0.22	0.11
$F_{DD}^t$	0.02	0.04	0.05	0.00	0.02
$F_{DD_a}^c$	0.21	0.13	0.12	0.22	0.15
$F_{RR}^c$	-0.19	-0.04	-0.06	0.05	0.06
$F_{RR}^t$	0.44	0.42	0.41	0.56	0.54
$F_\beta$	0.48	0.48	0.47	0.48	0.46
$F_\phi$	0.48	0.48	0.44	0.48	0.47
$F_\sigma$	0.48	0.41	0.38	0.48	0.41
$F_\Delta$		0.48	0.60		0.47
$F_{\beta\beta}^c$	0.00	0.00	0.00	-0.01	0.00
$F_{\beta\beta}^t$	-0.09	-0.11	-0.10	-0.08	-0.07
$F_{\phi\phi}^c$	-0.01	-0.02	-0.02	-0.04	-0.05
$F_{\phi\phi}^t$	0.09	0.07	0.10	0.08	0.07
$F_\alpha - F_{\alpha\alpha}^t$	0.57	0.49	0.65	0.50	0.59
$F_\psi - F_{\psi\psi}^t$	0.57	0.53	0.46	0.50	0.50
$F_\gamma - F_{\gamma\gamma}^t$	0.67	0.56	0.50	0.63	0.57
$F_\alpha - F_{\alpha\psi}^c$	0.57	0.53	0.60	0.50	0.46
$F_{\alpha\alpha}^c - F_{\alpha\psi}^c$	0.08	0.10	0.11	0.14	0.12
$F_{\alpha\alpha}^t - F_{\alpha\psi}^t$	-0.02	0.03	-0.05	0.13	0.11

<sup>a</sup> Units are  $\text{mdyn A}^{-1}$  for stretching and  $\text{mdyn A rad}^{-2}$  for bending coordinates. <sup>b</sup> See footnote *b* of Table X. <sup>c</sup>  $M(\text{CO})_6$  force constants (except CMC bending constants) from ref 2; CMC bending force constants from ref 5. <sup>d</sup> No errors estimated for force constants in FCOMPLY.

anticipated as the equatorial system should be only weakly perturbed by the substitution of an axial ligand. Indeed, the transferability of equatorial interaction compliants suggests that the final field is reliable.

**Bend-Bend Constants.** The valence potential constants for the bending modes of the  $M(\text{CO})_5(\text{CX})$  species are also shown in Tables X and XI. The equatorial constants,  $C_\beta$ ,  $C_\phi$ , and their interactions, all fall within the error limits of the corresponding hexacarbonyl values. Those constants which are defined solely in the E block, such as  $C_\Delta$ , are more poorly

determined than the rest owing to the complexity of this particular block. The uncertainties in  $C_\Delta$  and  $C_\sigma$  [MCX and MCO (axial) linear bending compliants, respectively] indicate that these constants may differ considerably from their true values. Nevertheless, the relative magnitudes of these constants and the corresponding MC(O) and MC(X) constants are similar, as expected, since increasing the strength of the MC(X) bond should increase the rigidity of the MCX fragment.

As in the case of the equatorial linear bending constants,

Table XII. Interaction Coordinates for the Stretching Modes of the  $M(\text{CO})_5(\text{CX})$  ( $X = \text{O}, \text{S}, \text{Se}$ ) Molecules<sup>a</sup>

$(j)_i = C_{i,j}/C_{i,i}$ <sup>c</sup>	$M(\text{CO})_6$ <sup>b</sup>	$\text{Cr}(\text{CO})_5$ - (CS)	$\text{Cr}(\text{CO})_5$ - (CSe)	$\text{W}(\text{CO})_5$ - (CS)
$(D)_D^c$	-0.0129	-0.0113	-0.0107	-0.0082
$(D)_D^t$	-0.0087	-0.0097	-0.0105	-0.0107
$(D)_{D_a} = (D_a)_D$	-0.0129	-0.0087	-0.0077	-0.0100
$(R)_{R_c}^c$	<i>d</i>	0.0118	0.0165	-0.0159
$(R)_{R_t}^t$	-0.228	-0.279	-0.278	-0.232
$(R)_{R_a}$	<i>d</i>	0.0044	0.0042	-0.0124
$(R)_{R_x}$	<i>d</i>	0.0053	0.0057	-0.0193
$(R_a)_{R_c} = (R_x)_{R_c}$	<i>d</i>	0.0045	0.0044	-0.0141
$(R_a)_{R_x}$	-0.228	-0.341	-0.367	-0.311
$(R_x)_{R_a}$	-0.228	-0.286	-0.269	-0.200
$(D)_{R_c}^c =$	-0.0446	-0.0402	-0.0395	-0.0494
$(D)_{R_c}^t =$	0.0040	0.0022	0.0022	0.0042
$(D_a)_{R_c} = (D_x)_{R_c}$				
$(D)_{R_c}^t$	0.019	0.0163	0.0160	0.0183
$(D)_{R_a}$	0.0040	0.0022	0.0020	0.0036
$(D)_{R_x}$	0.0040	0.0026	0.0028	0.0057
$(D_a)_{R_a}$	-0.00446	-0.0394	-0.0371	-0.0434
$(D_a)_{R_x}$	0.019	0.019	0.020	0.025
$(D_x)_{R_x}$	-0.0446	-0.0470	-0.0501	0.0673
$(D_x)_{R_a}$	0.019	0.0160	0.0151	0.0161
$(R)_D = (R_a)_D$	-0.401	-0.390	-0.390	-0.374
$(R)_D^c$	0.037	0.022	0.022	0.032
$(R)_D^t = (R_x)_D$	0.164	0.158	0.158	0.139
$(R)_D_a =$	0.037	0.038	0.038	0.030
$(R_a)_D = (R_x)_D$				
$(R)_D_x$	0.037	0.010	0.007	0.014
$(R_a)_D_x$	0.164	0.071	0.053	0.060
$(R_x)_D_x$	-0.401	-0.174	-0.131	-0.163

<sup>a</sup> The  $(j)_i$  are dimensionless for stretch-stretch interactions. <sup>b</sup>  $M(\text{CO})_6$  ( $M = \text{Cr}, \text{Mo}, \text{W}$ ) values are taken from ref 12. <sup>c</sup> The  $i$  and  $j$  refer to the internal coordinates given in Figure 2; the superscripts  $c$  and  $t$  represent cis and trans interactions, respectively, of the equatorial coordinates. <sup>d</sup> The MC cis interaction coordinates are not statistically equivalent in the three metal hexacarbonyls; this constant equals 0.0041 in the chromium complex and -0.0128 in the tungsten complex.<sup>12</sup>

the values for the CMC compliants are all within the error limits of the corresponding  $M(\text{CO})_6$  values.

**Interaction Coordinates.** Compliance constants are directly related to the interaction displacement coordinates,  $(j)_i$ , as shown by Jones.<sup>4</sup>  $(j)_i$  represent the relative displacement of coordinate  $j$  required to minimize the potential energy when coordinate  $i$  is distorted by a unit amount. Interaction coordinates are closely related to electronic structure and to the changes in electronic configuration which occur when a coordinate is displaced. The interaction coordinates for the stretch-stretch interactions of the  $M(\text{CO})_5(\text{CX})$  molecules are given in Table XII. On substitution of O by S or Se, the most dramatic change occurs in the  $[\text{MC}(\text{X})]_{\text{CX}}$  coordinate which represents the relative displacement of  $\text{MC}(\text{X})$  required to minimize the potential energy when  $\text{CX}$  is stretched a unit amount. The values obtained for this coordinate for  $X = \text{O}, \text{S}$ , and  $\text{Se}$  are -0.401 [ $M(\text{CO})_6$ , i.e., statistical average for  $M = \text{Cr}, \text{Mo}, \text{W}$ ], -0.174 [ $\text{Cr}(\text{CO})_5(\text{CS})$ ], and -0.131 [ $\text{Cr}(\text{CO})_5(\text{CSe})$ ]. This large variation in  $[\text{MC}(\text{X})]_{\text{CX}} [= C_{\text{CX},\text{MC}(\text{X})}/C_{\text{CX}}]$  is due to the substantial decrease in  $C_{\text{CX}}$  on descending the chalcocarbonyls since the interaction constants were constrained to the hexacarbonyl values. As mentioned above, we believe these to be reasonable constraints. Thus, the interaction coordinates themselves should give a reasonably good indication of the variations in the electronic structures of the complexes.

In an MCO group, the MC and CO interactions are usually interpreted in terms of  $\pi$  back-bonding only;<sup>2,4</sup> as the CO bond

is stretched, its  $\pi^*$  orbitals are more available for overlap with the metal  $d\pi$  electrons which results in a decrease in the MC bond length. Similar considerations predict interaction coordinates of the same magnitude, or even greater, for MCS and MCSe. The smaller values obtained for these groups suggest the involvement of two or more effects which partly cancel each other. It has been pointed out that the main difference between the CO and CS ligands is the relative instability of the occupied  $7\sigma$  and  $2\pi$  levels of CS.<sup>6</sup> Both of these levels were found to interact considerably with the metal center in  $\text{Cr}(\text{CO})_5(\text{CS})$ . Stretching the CS bond stabilizes the  $7\sigma$  level and increases the energy separation between this level and the  $\sigma$ -bonding orbitals of the metal, leading to reduced MC overlap. The  $2\pi$  levels, on the other hand, are destabilized as the CS bond is stretched and their carbon character reduced, which again decreases the MC overlap.

In MCS, these effects apparently cancel to some extent the effect of increased MC  $\pi$  overlap. Thus, the overall change in the MC bond order is reduced, and the interaction coordinate is decreased from its value in MCO. Such arguments should also apply to the CrCSe group, and the small difference in the  $[\text{MC}(\text{X})]_{\text{CX}}$  value for  $\text{Cr}(\text{CO})_5(\text{CS})$  and  $\text{Cr}(\text{CO})_5(\text{CSe})$  indicates, in accordance with the photoelectron spectra,<sup>20</sup> that the bonding in the CS and CSe ligands is quite similar.

The  $(\text{CX})_{\text{MC}(\text{X})}$  coordinates show the opposite trend as  $X$  is changed from O to S and then to Se. The values calculated in this case are -0.0403, -0.0470, and -0.0507 for  $\text{Cr}(\text{CO})_6$ ,  $\text{Cr}(\text{CO})_5(\text{CS})$ , and  $\text{Cr}(\text{CO})_5(\text{CSe})$ , respectively. Here again, the negative values of the coordinates are consistent with a simple  $d\pi$ - $p\pi^*$  bonding model; as the  $\text{MC}(\text{X})$  bond is stretched,  $\pi$  back-bonding from the metal is reduced and the adjacent CX bond decreases in length. The greater reduction predicted for the CS and CSe bond lengths is reasonable considering that the  $\pi^*$  orbitals of these ligands accept more electron density than those of CO.

It is also worth mentioning here that the weak Raman activity of the CS stretching mode has been accounted for by the mutual interactions of the CS  $\pi$  and  $\pi^*$  levels with the metal.<sup>6</sup> Stretching the CS bond increases the interaction of the  $\pi^*$  orbitals with the metal and also increases their carbon character. Conversely, the CS  $\pi$  levels are destabilized when the CS bond is stretched and they acquire less carbon character, thereby decreasing their interaction with the metal. These two competing effects reduce the change in polarizability of the CS group during its stretching vibration and weaken its Raman activity. The equally weak activity of the  $\nu(\text{CSe})$  mode is further support for the similarity of the CS and CSe ligands.

**Potential Energy Distribution for the  $M(\text{CO})_5(\text{CX})$  Molecules.** Table XIII lists the contributions of the symmetry coordinates ( $V_{ij,k}$ ) to the potential energy of the normal modes of the  $M(\text{CO})_5(\text{CX})$  molecules. A comparison of the PED's of the  $M(\text{CO})_6$  ( $O_h$ ) and  $M(\text{CO})_5(\text{CX})$  ( $C_{4v}$ ) molecules is possible by comparing the contributions from the coordinates in the  $A_1$ ,  $B_1$ , and  $B_2$  blocks of the  $C_{4v}$  systems with those of the analogous coordinates in the  $A_{1g} + T_{1u}$ ,  $E_g + T_{2u}$ , and  $T_{2g}$  blocks, respectively, of the  $O_h$  systems. The various  $V_{ij,k}$  for the two systems agree closely; in particular, the PED's for the  $B_1$  and  $B_2$  blocks are almost identical with their  $M(\text{CO})_6$  equivalents since all the  $C_{i,j}$  ( $i \neq j$ ) in these blocks were constrained at their  $M(\text{CO})_6$  values. In the E block, however, there is so much mixing of coordinates forbidden under  $O_h$  symmetry, that many of the  $V_{ij,k}$  do not have hexacarbonyl equivalents.

In the  $A_1$  blocks, all the complexes show appreciable mixing between the equatorial and axial CO stretches but none be-

(20) A. M. English, K. R. Plowman, I. S. Butler, E. Diemann, and A. Müller, *Inorg. Chim. Acta*, **32**, 113 (1979).

**Table XIII.** Diagonal Elements of the Potential Energy Distribution for the Normal Isotopic  $M(\text{CO})_5(\text{CX})$  Species<sup>a-d</sup>

		$\text{Cr}(\text{CO})_5(\text{CS})$				$\text{W}(\text{CO})_5(\text{CS})$		
a <sub>1</sub>	$\nu_1$	$0.78S_1 + 0.18S_2$		b <sub>2</sub>	$\nu_{14}$	$0.44S_{14} + 0.29S_{15}$		
	$\nu_2$	$0.20S_1 + 0.82S_2$			$\nu_{15}$	$0.71S_{14} + 0.88S_{15}$		
	$\nu_3$	$0.89S_3 + 0.18S_7$			e	$\nu_{16}$	$1.02S_{16}$	
	$\nu_4$	$0.37S_4 + 0.11S_5 + 0.25S_8$				$\nu_{17}$	$0.23S_{17} + 0.17S_{19}$	
	$\nu_5$	$0.18S_3 + 0.63S_5 + 0.21S_7$				$\nu_{18}$	$0.10S_{17} + 0.22S_{18} + 0.14S_{20} + 0.18S_{22}$	
	$\nu_6$	$0.93S_6$				$\nu_{19}$	$0.36S_{17} + 0.17S_{21} + 0.11S_{24}$	
	$\nu_7$	$0.10S_3 + 0.21S_5 + 0.46S_7$				$\nu_{20}$	$0.60S_{19} + 0.11S_{20}$	
	$\nu_8$	$0.69S_4 + 0.19S_5 + 0.25S_7 + 1.04S_8$				$\nu_{21}$	$0.48S_{18} + 0.32S_{20} + 0.32S_{21}$	
b <sub>1</sub>	$\nu_{10}$	$1.00S_{10}$		$\nu_{22}$		$0.23S_{17} + 0.12S_{18} + 0.21S_{19} + 0.36S_{20} + 0.50S_{22} + 0.27S_{23}$		
	$\nu_{11}$	$0.78S_{11}$		$\nu_{23}$		$0.22S_{17} + 0.14S_{18} + 0.10S_{20} + 0.15S_{21} + 0.38S_{22} + 0.67S_{23}$		
	$\nu_{12}$	$0.96S_{12}$		$\nu_{24}$	$0.39S_{21} + 0.10S_{22} + 0.20S_{23} + 0.90S_{24}$			
	$\nu_{13}$	$0.26S_{11} + 0.97S_{13}$						
b <sub>2</sub>	$\nu_{14}$	$0.44S_{14} + 0.29S_{15}$						
	$\nu_{15}$	$0.71S_{14} + 0.86S_{15}$						
e	$\nu_{16}$	$1.02S_{16}$						
	$\nu_{17}$	$0.29S_{17} + 0.16S_{19} + 0.11S_{23}$						
	$\nu_{18}$	$0.34S_{18} + 0.12S_{20} + 0.15S_{22} + 0.12S_{24}$						
	$\nu_{19}$	$0.38S_{17} + 0.11S_{19} + 0.13S_{20} + 0.10S_{21}$						
	$\nu_{20}$	$0.56S_{19} + 0.16S_{20}$						
	$\nu_{21}$	$0.41S_{18} + 0.27S_{20} + 0.39S_{21}$						
	$\nu_{22}$	$0.36S_{17} + 0.25S_{19} + 0.24S_{20} + 0.33S_{22} + 0.47S_{23}$						
	$\nu_{23}$	$0.12S_{17} + 0.22S_{18} + 0.15S_{20} + 0.21S_{21} + 0.47S_{22} + 0.34S_{23} + 0.16S_{24}$						
$\nu_{24}$	$0.30S_{21} + 0.19S_{22} + 0.35S_{23} + 0.80S_{24}$							
a <sub>1</sub>	$\nu_1$	$0.78S_1 + 0.20S_2$		b <sub>2</sub>	$\nu_{14}$	$0.57S_{14} + 0.21S_{15}$		
	$\nu_2$	$0.21S_1 + 0.81S_2$			$\nu_{15}$	$0.55S_{14} + 0.91S_{15}$		
	$\nu_3$	$0.75S_3 + 0.32S_7$			e	$\nu_{16}$	$1.03S_{16}$	
	$\nu_4$	$0.38S_4 + 0.10S_5 + 0.25S_8$				$\nu_{17}$	$0.33S_{17}$	
	$\nu_5$	$0.16S_4 + 0.72S_5 + 0.12S_7$				$\nu_{18}$	$0.19S_{17} + 0.13S_{18} + 0.28S_{20} + 0.15S_{22}$	
	$\nu_6$	$0.96S_6$				$\nu_{19}$	$0.28S_{18} + 0.20S_{21} + 0.20S_{24}$	
	$\nu_7$	$0.21S_3 + 0.15S_5 + 0.39S_7$				$\nu_{20}$	$0.94S_{19}$	
	$\nu_8$	$0.66S_4 + 0.17S_5 + 0.32S_7 + 1.02S_8$				$\nu_{21}$	$0.39S_{18} + 0.30S_{20} + 0.38S_{21}$	
b <sub>1</sub>	$\nu_{10}$	$1.00S_{10}$		$\nu_{22}$		$0.23S_{17} + 0.16S_{18} + 0.46S_{20} + 0.78S_{22} + 0.13S_{23}$		
	$\nu_{11}$	$0.80S_{11}$		$\nu_{23}$		$0.45S_{17} + 0.24S_{21} + 0.20S_{22} + 0.85S_{23} + 0.15S_{24}$		
	$\nu_{12}$	$0.96S_{12}$		$\nu_{24}$	$0.35S_{21} + 0.16S_{22} + 0.41S_{23} + 0.89S_{24}$			
	$\nu_{13}$	$0.26S_{11} + 0.96S_{13}$						

<sup>a</sup> The symmetry coordinates  $S_i$  are defined in Table IV. <sup>b</sup> The coefficients of  $S_i$ ,  $V_{ii,h}$ , give the contribution of  $S_i$  to the normal mode  $\nu_k$ . <sup>c</sup> Contributions less than 0.10 are omitted. <sup>d</sup> The major contribution to a mixed mode is underlined.

tween the CO and CS stretching modes. The mixing of  $\nu(\text{CX})$  and  $\nu[\text{MC}(\text{X})]$  increases progressively as O is replaced by S and Se. Also,  $\nu[\text{MC}(\text{O})]$  (axial) and  $\nu[\text{MC}(\text{X})]$  are extensively mixed, whereas the equatorial MC stretch is essentially uncoupled.

Strong mixing of the MCO and CMC bends is observed for all the blocks, and, in the chromium complexes, these modes also show a significant amount of MC stretching. In the E block, the linear bending modes are highly mixed, particularly the MCO and MCX axial bends and the equatorial out-of-plane bends. In fact, most of the modes in the block are so strongly coupled that only the  $\nu(\text{CO})$ ,  $\nu(\text{MC})$ , and  $\delta(\text{CMC})$  ( $\nu_{24}$ ) modes should be assigned characteristic frequencies.

**Eigenvectors for the a<sub>1</sub> Modes.** Table XIV (supplementary material) lists the eigenvectors for the a<sub>1</sub> fundamental modes of unlabeled  $\text{Cr}(\text{CO})_5(\text{CS})$  only since these vectors are very similar for all three complexes. In particular,  $L_{1,1}$ ,  $L_{1,2}$ , and  $L_{2,2}$  are identical. Furthermore, their ratios ( $-L_{1,2}/L_{1,1} = L_{2,1}/L_{2,2} = 1/2$ ) have the values which, according to Bigorne,<sup>2</sup> should give rise to a highly polarized band for  $\nu_1$  and a depolarized band for  $\nu_2$ , as observed for  $\text{Cr}(\text{CO})_5(\text{CS})$  but not  $\text{W}(\text{CO})_5(\text{CS})$ .

**Energy-Factored Force Fields (EFFF).** Anharmonic en-

ergy-factored force fields were determined for the  $\text{M}(\text{CO})_5(\text{CX})$  species as an aid to the assignment of the partially labeled species and to determine the position of the IR-inactive  $\nu(\text{CO})$  b<sub>1</sub> mode, as discussed above. The frequencies calculated by the anharmonic EFFF are given in supplementary Table Ia for the vapour spectra of  $\text{Cr}(\text{CO})_5(\text{CX})$  and the final force constants are given in Table XV. Harmonic EFFF were obtained from the harmonic  $\nu(\text{CO})$  and  $\nu(\text{CX})$  frequencies for  $\text{Cr}(\text{CO})_5(\text{CX})$  and  $\text{W}(\text{CO})_5(\text{CS})$ <sup>3</sup> to allow a comparison of the harmonic CO and CX energy-factored force constants with those obtained with use of the GQVFF. The CX force constants in Table XV were determined from the corresponding CX frequencies with all (CO,CX) interactions being set equal to zero.

As in the case of  $\text{M}(\text{CO})_6$ ,<sup>2</sup> the neglect of anharmonicity corrections has a significant effect on the primary CO stretching force constants and the (CO,CO) trans interaction constants, the cis interaction constants changing to a lesser extent. CO-energy factoring, on the other hand, leads to large errors for all the interaction constants, but, again, the trans (CO,CO) constant is the one most affected. Similar results were obtained for the CO-EFFF of the metal hexacarbonyls<sup>2</sup> and  $\text{Mn}(\text{CO})_5\text{Br}$ .<sup>11</sup>

**Table XV.** CO and CX Force Constants and (CO,CO) Interaction Constants for the  $M(\text{CO})_5(\text{CX})$  Molecules for Various Force Fields

Cr(CO) <sub>5</sub> (CS)					
F <sup>a</sup>	soln <sup>b</sup>		vapor <sup>c</sup>		vapor har GQ <sup>d</sup>
	anhar	EF	anhar	EF	
F <sub>D</sub>	16.46	16.68	16.71	17.19	17.28
F <sub>D<sub>a</sub></sub>	16.63	16.91	17.01	17.30	17.42
F <sub>DD<sup>c</sup></sub>	0.24	0.23	0.21	0.24	0.18
F <sub>DD<sup>t</sup></sub>	0.47	0.39	0.21	0.30	0.04
F <sub>DD<sub>a</sub></sub>	0.22	0.22	0.21	0.17	0.13
F <sub>D<sub>x</sub></sub>	8.18	8.41	8.01	8.52	7.68
Cr(CO) <sub>5</sub> (CSe)					
F <sup>a</sup>	soln		vapor		vapor har GQ
	anhar	EF	anhar	EF	
F <sub>D</sub>	16.50	16.71	17.19	17.19	17.28
F <sub>D<sub>a</sub></sub>	16.72	16.98	17.34	17.34	17.47
F <sub>DD<sup>c</sup></sub>	0.23	0.23	0.22	0.22	0.16
F <sub>DD<sup>t</sup></sub>	0.46	0.39	0.30	0.30	0.05
F <sub>DD<sub>a</sub></sub>	0.20	0.20	0.16	0.16	0.12
F <sub>D<sub>x</sub></sub>	7.13	7.38	7.42	7.42	5.77
W(CO) <sub>5</sub> (CS)					
F <sup>a</sup>	vapor		vapor <sup>e</sup>		vapor har GQ
	anhar	EF	anhar	EF	
F <sub>D</sub>	16.71	16.78	17.16	17.16	17.28
F <sub>D<sub>a</sub></sub>	16.60	16.88	17.08	17.08	17.24
F <sub>DD<sup>c</sup></sub>	0.27	0.16	0.25	0.25	0.11
F <sub>DD<sup>t</sup></sub>	0.47	0.12	0.37	0.37	0.02
F <sub>DD<sub>a</sub></sub>	0.21	0.16	0.21	0.21	0.15
F <sub>D<sub>x</sub></sub>	8.50	8.17	8.61	8.61	7.46

<sup>a</sup> Subscripts and superscripts are explained in footnote *a* of Table V. Units: mdyn Å<sup>-1</sup>. <sup>b</sup> CS<sub>2</sub> solution; EF = energy factored. <sup>c</sup> The values calculated here for the interaction constants are considered more reasonable than those given previously.<sup>5</sup> <sup>d</sup> GQ = general quadratic. <sup>e</sup> Force constants from ref 5.

A comparison of the CX energy-factored force constants and the corresponding general quadratic constants indicates that energy factoring is a poor approximation for the  $\nu(\text{CS})$  and  $\nu(\text{CSe})$  modes. If one examines the expression for the  $\nu(\text{CX})$  mode of an isolated MCX (X = O, S, Se) moiety, it becomes obvious why energy factoring is an increasingly poor approximation as O is replaced by S or Se (Table XV).

Labeling the CX and MC(X) stretches, coordinates 1 and 2, respectively, the secular equation for this two-coordinate system is given by eq 1 which yields eq 2 for  $\lambda_1$  after matrix

$$\begin{bmatrix} G_{1,1}F_{1,1} + G_{1,2}F_{1,2} & G_{1,1}F_{1,2} + G_{1,2}F_{2,2} \\ G_{1,2}F_{1,1} + G_{2,2}F_{1,2} & G_{1,2}F_{1,2} + G_{2,2}F_{2,2} \end{bmatrix} \begin{bmatrix} L_{1,1} & L_{1,2} \\ L_{2,1} & L_{2,2} \end{bmatrix} = \begin{bmatrix} L_{1,1} & L_{1,2} \\ L_{2,1} & L_{2,2} \end{bmatrix} \begin{bmatrix} \lambda_1 & \\ & \lambda_2 \end{bmatrix} \quad (1)$$

$$\lambda_1 = G_{1,1}F_{1,1} + (G_{1,2}F_{1,2}) + (G_{1,1}F_{1,2} + G_{1,2}F_{2,2})L_{2,1}/L_{1,1} \quad (2)$$

multiplication. For an isolated CX stretch,  $\lambda_1$  is simply given by eq 3.

$$\lambda_1 = G_{1,1}F_{1,1} \quad (3)$$

If the values obtained for  $F_{2,2}$  and  $L_{2,1}$  are substituted into eq 2, a comparison of the energy-factored (eq 2)  $F_{1,1}$  values arising from a given  $\lambda_1$  value is possible. From Table XIV,  $L_{2,1}/L_{1,1}$  for  $\text{Cr}(\text{CO})_5(\text{CS})$  and  $\text{Cr}(\text{CO})_5(\text{CSe})$  were found to be  $-0.79$  and  $-0.97$ , respectively, while a value of  $-0.581$  was previously calculated for this ratio in an isolated MCO sys-

**Table XVI.** Harmonic Frequencies (cm<sup>-1</sup>) and Harmonic Force Constants (mdyn Å<sup>-1</sup>) for Free and Coordinated CX (X = O, S, Se) Ligands

ligand	molecule <sup>a</sup>	F <sub>CX</sub>	$\omega_e$
CO	CO	19.017	2169.8
CO	Cr(CO) <sub>6</sub>	17.24	2060.1 <sup>b</sup>
CO	W(CO) <sub>6</sub>	17.22	2056.9 <sup>b</sup>
CS	CS	8.489	1285.1
CS	Cr(CO) <sub>5</sub> (CS)	7.68	1287.3
CS	W(CO) <sub>5</sub> (CS)	7.46	1294
CSe	CSe	6.587	1036.0
CSe	Cr(CO) <sub>5</sub> (CSe)	5.77	1098

<sup>a</sup> Vapor phase data used for all molecules;  $\text{M}(\text{CO})_6$  and diatomic data from ref 2 and 4, respectively. <sup>b</sup> Arithmetic mean of  $a_{1g}$ ,  $e_g$ , and  $t_{1u}$   $\nu(\text{CO})$  frequencies weighted by their degeneracies.

tem.<sup>21</sup> Thus, bearing in mind that  $G_{1,1} = (\mu_{\text{CX}})^{-1}$  and  $G_{1,2} = -\mu_{\text{C}}$ ,  $F_{\text{MC}(\text{O})} < F_{\text{MC}(\text{S})} < F_{\text{MC}(\text{Se})}$  (Table XI), and bearing in mind that under the constraints employed in the general quadratic calculations the values obtained for  $F_{1,2}$  increase in the order  $F_{\text{CO,MC}} > F_{\text{CS,MC}} > F_{\text{CSe,MC}} > 0$ <sup>22</sup> it is evident that the terms  $(G_{1,2}F_{1,2})$  and  $[(G_{1,1}F_{1,2} + G_{1,2}F_{2,2})L_{2,1}/L_{1,1}]$  of eq 2 become less negative and more positive, respectively, upon descending the O, S, Se series. The relatively close agreement of the energy-factored and general quadratic force constants for CO stretching modes (Table XV) is due to the fortuitous canceling of the extra terms in eq 2 for the carbonyl group. For the thio- and selenocarbonyls, the sum of these terms is greater than zero by increasing amounts, and the general quadratic force constants decrease in value relative to the corresponding energy-factored constants.

The  $L_{2,1}/L_{1,1}$  ratio gives the relative amplitudes of MC and CX bond displacements in the normal mode assigned to the CX stretch. Thus, the large increase in the absolute value of this ratio signifies a greater degree of coupling between these two motions as the atomic weight of X increases. Furthermore, the considerable effect of  $L_{2,1}/L_{1,1}$  on the size of the last term in eq 2 explains how increased mixing prevents changes in the observed CX frequencies from accurately reflecting changes in the CX bond orders on coordination since both  $\nu(\text{CS})$  and  $\nu(\text{CSe})$  may increase in frequency relative to the free ligand while  $F_{\text{CS}}$  and  $F_{\text{CSe}}$  decrease. Table XVI, which lists force constants and wavenumbers for the coordinated and free chalcocarbonyl ligands, emphasizes this point dramatically.

**Acknowledgment.** This work was generously supported by the Natural Sciences and Engineering Research Council of Canada and the Gouvernement du Quebec (Ministere de l'Education).

**Registry No.** Cr(CO)<sub>5</sub>(CS), 50358-90-2; Cr(<sup>13</sup>CO)<sub>5</sub>(CS), 77450-25-0; Cr(CO)<sub>5</sub>(<sup>13</sup>CS), 77450-26-1; Cr(CO)<sub>5</sub>(CSe), 63356-87-6; Cr(<sup>13</sup>CO)<sub>5</sub>(CSe), 77450-27-2; W(CO)<sub>5</sub>(CS), 50358-92-4; *trans*-W(CO)<sub>4</sub>(<sup>13</sup>CO)(CS), 60172-96-5; *cis*-Cr(CO)<sub>4</sub>(<sup>13</sup>CO)(CS), 77450-15-8; *cis*-Cr(<sup>13</sup>CO)<sub>4</sub>(CO)(CS), 77450-16-9; *trans*-Cr(<sup>13</sup>CO)<sub>4</sub>(CO)(CS), 77481-56-2; *cis*-Cr(CO)<sub>4</sub>(<sup>13</sup>CO)(CSe), 77450-17-0; *cis*-Cr(<sup>13</sup>CO)<sub>4</sub>(CO)(CSe), 77450-18-1; *trans*-Cr(<sup>13</sup>CO)<sub>4</sub>(CO)(CSe), 77481-57-3.

**Supplementary Material Available:** Observed and calculated wavenumbers for the  $\nu(\text{CO})$  modes of  $\text{Cr}(\text{CO})_n(\text{CO})_{5-n}(\text{CX})$  species in the vapor phase (supplementary Table Ia) and Table XIV [a more comprehensive listing of the  $a_1$  fundamentals of the  $\text{M}(\text{CO})_5(\text{CO})_n(\text{CX})$  molecules] (4 pages). Copies of the actual spectra for the various species studied in this work are available from the authors upon request. Ordering information is given on any current masthead page.

(21) P. S. Braterman, "Metal Carbonyl Spectra", Academic Press, London, 1975.

(22) It should be noted that constraining a given compliant is not equivalent to constraining the corresponding force constant, e.g.,  $F_{\text{CX,MC}(\text{X})} = 0.68, 0.36,$  and  $0.30$  mdyn Å<sup>-1</sup> in  $\text{Cr}(\text{CO})_6, \text{Cr}(\text{CO})_5(\text{CS}),$  and  $\text{Cr}(\text{CO})_5(\text{CSe})$ , respectively.